UCRL -2435 Rev.
Cy. 2

UNIVERSITY OF CALIFORNIA

Ernest O. Lawrence Radiation Laboratory

BERKELEY, CALIFORNIA

DISCLAIMER

UCRL-2435 Rev.

UNIVERSITY OF CALIFORNIA
Radiation Laboratory
Berkeley, California

Contract No. W-7405-eng-48

THE SECOND ELECTRON MODEL PHASE-COMPENSATED C-W CYCLOTRON

March, 1955

WORK DONE BY:

Elmer Kelly
J. R. Richardson
Robert V. Pyle
Robert L. Thornton
K. R. MacKenzie

REPORT WRITTEN BY:

Robert Pyle

UCRL-2435 Rev.
Unclassified Physics

THE SECOND ELECTRON MODEL PHASE-COMPENSATED C-W CYCLOTRON

Robert Pyle

March, 1955

THE SECOND ELECTRON MODEL PHASE-COMPENSATED C-W CYCLOTRON

Robert Pyle

Table of Contents

THE SECOND ELECTRON MODEL PHASE-COMPENSATED C-W CYCLOTRON

Robert Pyle

Radiation Laboratory, Department of Physics
University of California, Berkeley, California

March, 1955

ABSTRACT

A 40-1/2-inch-diameter constant-frequency cyclotron was built which accelerated electrons to v/c = 0.51. It was an improved version of the model described in UCRL-2344 and based on the idea of L. H. Thomas.* An azimuthal variation in the magnetic field makes the periods of revolution the same in all stable orbits, and provides suitable axial and radial focusing properties.

The analytical expression for the magnetic field at the median plane is

$$H_z\Big|_{z=0} = H_0\left[1 + A\left(\frac{\omega r}{c}\right)\cos 3\theta + B\left(\frac{\omega r}{c}\right)^2 + C\left(\frac{\omega r}{c}\right)^3 \cos 3\theta + D\left(\frac{\omega r}{c}\right)^4 + E\left(\frac{\omega r}{c}\right)^5 \cos 3\theta + F\left(\frac{\omega r}{c}\right)^6\right]$$

where

A = 1.3000	$\omega = 2\pi f = 2\pi\ 54.1$ mc
B = 0.2888	H_0 = 19.3 gauss
C = 0.8000	r = radius in inches
D = 0.1153	θ = azimuthal coordinate
E = 0	
F = 0.4175	

Three 60°-wide wedge-shaped "triants," located at the azimuths of minimum magnetic field, were used as accelerating electrodes. When driven 120° out of phase, these electrodes gave a calculated energy gain per turn of $3e\,V_0$, where V_0 is the peak triant-to-ground voltage. Electrons were accelerated to v/c = 0.50 with V_0 = 23 volts. This "threshold" voltage was set by the geometry of the source structure, rather than by the magnetic field.

---

*L. H. Thomas, Phys. Rev. 54, 580 (1938).

The axial focusing was sufficient to prevent axial loss of electrons at radii larger than 5 inches. The radial instability predicted for the velocity at which the frequency of the radial oscillation is three-halves the cyclotron frequency was observed. The energy at which this radial instability occurred could be changed by slightly altering the shape of the magnetic field.

THE SECOND ELECTRON MODEL PHASE-COMPENSATED C-W CYCLOTRON

Robert Pyle

Radiation Laboratory, Department of Physics
University of California, Berkeley, California

March, 1955

INTRODUCTION

The behavior of the first model of the cyclotron based on the idea of L. H. Thomas[1] (see UCRL-2344) was sufficiently encouraging that construction was begun on a second electron model in the Spring of 1952. By that time the theoretical aspects of the design problem had been extensively investigated by David Judd and Richard Huddlestone, and engineering studies for the design of a full-scale 300-Mev deuteron machine were nearing completion. The new model cyclotron was therefore an engineering model, similar in all possible respects to the proposed deuteron machine, and at the same time a device for testing such aspects of the theory as the previous model was unsuited for. The main points for investigation were felt to be (a) the threshold voltage, and (b) the behavior of the circulating electrons at energies near the theoretical upper limit.

The experimental results showed that the cyclotron behaved very much as predicted by the theoretical group, and was capable of satisfactorily accelerating electrons, without axial loss, to a velocity 0.51 that of light.

---

[1] L. H. Thomas, Phys. Rev. 54, 580 (1938).

THEORY

The principles upon which this cyclotron was based were briefly discussed in the report covering the previous model (UCRL-2344). The factors considered in choosing the exact shape of the magnetic field are covered in Appendix I of this paper.

The theoretical expression for the magnetic field is in the form of an infinite series:

$$H_z\Big|_{z=0} = H_0 \left[(1 + A(\omega r/c)\cos 3\theta + B(\omega r/c)^2 + C(\omega r/c)^3 \cos 3\theta + D(\omega r/c)^4 + E(\omega r/c)^5 \cos 3\theta + F(\omega r/c)^6 + \ldots\ldots \right]$$

where: A = 1.300, B = 0.2888, C = 0.800, D = 0.1153, E = 0, and F = 0.4175; $\omega = 2\pi f = 2\pi\ 54.1/\text{Mc}$, H_0 = 19.3 gauss, r = the radius in inches, and θ is the azimuthal coordinate.

The coefficients were chosen to give the optimum axial and radial focusing, while keeping the particles in phase with the accelerating voltage. The number of terms used was that given in the above expression. This series converges rather slowly at the higher velocities, and the effect of higher-order terms was included to some extent by adjusting the coefficients to make the error in the period of revolution less than 0.1 percent for all orbits.

A compromise must be made when choosing the axial and radial restoring forces. The frequency of the radial oscillations increases with increasing energy until the velocity is reached at which one-half of a radial oscillation is completed in one-third of a revolution. The theory shows that for larger speeds the orbit is radially unstable, and in fact the amplitude of this oscillation grows exponentially as energy is supplied.

It was shown theoretically that the larger the axial restoring force, the lower the velocity at which the radial instability commences. The maximum energy obtainable is determined by setting the axial restoring force equal to zero at all radii. For a somewhat different geometry, McMillan found this upper limit is reached at a value of v/c of about 0.55. The maximum energy is believed to be somewhat lower for a cyclotron. However, it would be impossible to accelerate a large current without substantial axial focusing, so the practical upper limit is reduced to a value of v/c of perhaps 0.52.

A second phenomenon occurs when $\frac{\omega_r}{\omega_0} = 3/2$: the radial oscillations become sorted in phase so that all particles have their maximum radial excursions at the same azimuth in the cyclotron. It appeared that it might be easier to extract the beam after this condition was reached, so for this reason, and as a check on the theoretical prediction of where the radial instability should set in, the constants in the magnetic field expansion were chosen so that the $\frac{\omega_r}{\omega_0} = 3/2$ point would be reached at $v/c = 0.490$, well within the cyclotron. Once these matters were checked, the magnetic field was to be adjusted to produce the maximum-energy beam that could be obtained without axial loss.

Calculated values of v/c and energy are tabulated for a number of radii in Table I. (See Appendix II, UCRL-2344 for method.)

Table I

Max. Radius (0°, 120°, 240°)	Min. Radius (60°, 180°, 300°)	v/c	Electron Energy (Kev)	Deuteron Energy for Same v/c (Mev)
3"	2.9	0.0855	1.90	
4"	3.9	0.1136	3.29	
5"	4.8	0.1415	5.21	
6"	5.7	0.1690	7.46	
7"	6.6	0.1964	10.12	
8"	7.5	0.2235	13.24	
9"	8.3	0.2505	16.81	
10"	9.1	0.2774	20.80	
11"	9.9	0.3040	25.35	
12"	10.8	0.3304	30.40	
13"	11.6	0.3568	35.97	
14"	12.4	0.3830	42.2	
15"	13.1	0.4091	48.9	
16"	13.8	0.4348	56.5	
17"	14.5	0.4604	64.6	235
18"	15.3	0.486	73.8	270
19"	16.0	0.5115	83.6	305
20"	16.8	0.5368	94.6	345

CONSTRUCTION

From the operation of the previous model, it was clear that one requirement for successful operation is that all surfaces that can be seen by the beam be good conductors. If nonconducting layers were deposited on the electrodes or ground sheets they would become charged and severely limit the operation of the cyclotron. This consideration was responsible for many of the constructional details:

Mercury rather than oil pumps were used.

"Molykote" rather than grease was used on all seals.

All internal rf cables were of teflon construction.

No tape or other material that might outgas was used in the vacuum tank. In spite of these precautions, a nonconducting layer was slowly laid down on surfaces struck by stray beam on the first turn or so. This material may have come from the emitting material of the source.

Poles

The design studies suggested a diameter of 324 in. for a cyclotron that would produce 300-Mev deuterons. The electron model was built to 1/8 scale, i.e., the diameter was 40.5 in. David L. Judd of the Theoretical Group was able to set up and solve a boundary-value potential problem that predicted the pole-face contours required to give the desired magnetic field in the median plane, assuming the iron to be an equipotential surface. The magnet group then approximated this surface with a series of level steps of various heights. Such an arrangement is much easier to machine and to shim than a smoothly contoured pole such as was used on the previous model.

The poles were constructed of Armco iron. Four discs of iron were used in each pole. (See Fig. 4 for dimensions.) The outermost two were flat disks, and the next one in was uncontoured except for some deep notches cut at the valley points (Fig. 1). The disk next to the median plane was cut into sixty-degree sections, which had the contours milled into them (Fig. 2). The outermost sections of these sectors were made removable to facilitate the machining of beam-extraction channels. One of the completely assembled poles is shown in Fig. 3.[2]

---

[2]Further constructional details are given in Assembly drawing 6B5995.

The lower pole is shown in the vacuum tank in Fig. 5. The minimum magnet gap when the poles were in the operating position was 1.825 inches; the minimum gap near the center of the cyclotron was 3.2 inches. The return path for the magnetic flux was through the air rather than through an iron yoke.

Magnet Coils

The poles were energized by two coils, each of which contained 3940 turns of no. 21 copper wire. They were mounted inside the main tank in vacuum-tight cans. Provision was made for air cooling them, but this proved to be unnecessary. One of the coils is shown in place in Fig. 5. The magnet gap and coil current were adjusted until the minimum amount of shimming was necessary; the current required turned out to be 77 ma. This current was supplied by a rectifier and electronic regulator which maintained (a) the current through the coils to 0.01 percent; or (b) the field at a magnetometer placed in the gap to the same precision.

Vacuum System

The vacuum tank was constructed of aluminum alloy. The general form can be seen in Figs. 5 and 6. The tank was 28 in. high, 80 in. wide, and 100 in. long, with the poles located near one end to provide space for external beam-focusing studies. All pump connections were made to the manifold shown in Fig. 7. The system was roughed through a 6-in. line by a 103-cfm Kinney pump and the hydraulically operated gates shown in Fig. 7 were then opened to the two 10-in. DPI mercury diffusion pumps. The latter were backed through a 4-in. line by a 43-cfm Kinney pump. Each diffusion pump was baffled by a refrigerated disk operated at -30° C and by a liquid-N_2 baffle. The liquid-N_2 traps were automatically filled and there was an automatic changeover to the second can when the first became empty. Safety devices were included so that the gates immediately closed upon any failure of the pumps or baffling system, or upon a pressure rise in the vacuum tank.

To prevent pump oil from getting into the vacuum tank, a large liquid-N_2 trap was provided in the roughing line. The forevac line had a trap containing a trichlorethylene-solid CO_2 mixture, which condensed oil and mercury vapors.

With this system the total pumpdown time to the operating pressure of 3×10^{-5} mm Hg was about one hour. The measured pumping speed for the whole system was 500 l./sec at this pressure.

Although the magnet poles formed part of the vacuum system, they were not supported by the tank. The lower pole rested on a pedestal set in the concrete floor. The weight of upper pole and the vacuum loading were carried by three stainless steel stanchions set just outside the coil cans. Two of these can be seen in Fig. 16.

Magnetic Field Measurements

The original intention was to shim the poles until the measured field at the geometrical median plane was everywhere within 0.1 percent of the design field. The field-measuring device was a magnetometer capable of measuring the model fields with a maximum error of 0.05 percent (See Appendix II for construction). The magnetometer head (Fig. 8) was mounted on an arm pivoted at the center of the cyclotron and supported by a track outside the poles (Fig. 13). Radial and azimuthal drive of the magnetometer carriage was provided by two motors mounted above the top pole. It was shown that the presence of these motors (which were not there when the cyclotron was running) changed the magnitude of the field by 0.4 percent but did not affect the field distribution.

The cyclotron was located in a building, which also housed two large electromagnets. Precise measurements and operation were possible only when they were off. Even the 184-inch synchrocyclotron, some 200 feet away, produced a gradient of 0.2 percent along a diameter. The electron model could not be shielded from these external fields by covering the tank with iron, because to do so would greatly increase the effects of residual magnetism in the poles.

After annealing, the poles still produced moderately large remnant fields which were further reduced by pounding the iron with an air hammer. The distribution of the residual magnetic field was changed if the current through the energizing coils changed abruptly, so that it was found desirable to use a motor-driven rheostat to slowly raise and lower the field. In addition, the magnetic condition of the iron was periodically restored to that which existed at the time of field measurement by running it through a program of decreasing hysteresis loops. The peak field required was five times the operating field. With these precautions the field could be reset to the desired accuracy.

After the initial gross shimming, the field was carefully measured, the data being taken on a Speedomax recorder. A second magnetometer at a fixed position in the gap was used as a monitor. The field at this time was within 1 percent of the desired value over most of the gap. New shims were then computed and installed, and the field remeasured. The cyclotron was put into operation before these data had been reduced.

A few additional field measurements were made after the cyclotron was shut down. These are discussed in the section on the Magnetic Field.

The Magnetic Field

Calculated magnetic-field contour lines, in percent of central field (19.3 gauss), are shown in Fig. 9. Also shown are some of the calculated stable orbits.

When the magnetic field was measured, a continuous record of the azimuthal variation of the magnetic field was obtained at radial intervals of one inch, through the 19-inch radius. The results are shown in Fig. 10, where the difference between the measured and theoretical fields is given. From these data the general observation can be made that when the magnet current was set to give the correct field at intermediate radii, the field was up to 1 percent too high at small radii, while for the last stable orbit the field was 1 percent too low at places on the hills* and 2 percent too high in patches in the valleys.

The field was clearly far from the 0.1 percent maximum error originally hoped for. The average fields over the orbits were undoubtedly much improved by the auxiliary coils (see the following section). The optimum field was not measured, but some information about the field corrections produced by the trimming coils is given in Appendix III.

It would appear that the 0.1 percent field tolerance could be achieved in the absence of variable stray fields with perhaps two further sets of shimming and field measurements, but at the low field strengths involved the time and care required would be very great.

The magnetic field measurements were made with the tank open, so that this gap had to be reproduced when the tank was at operating pressure.

---

*"Hills" and "valleys" are regions where the magnetic fields are large and small, respectively (see for example Fig. 13). In the expression for the magnetic field $\theta = 0^{\circ}$ is a hill and $\theta = 60^{\circ}$ is a valley.

Dial indicators could be rotated into the gap to measure the spacing between poles, and it was found that the magnet gap was reduced 14 mils when the tank was pumped down. The stanchions were then shimmed until the gaps were correct under vacuum loading. This measurement was repeated at frequent intervals.

Auxiliary Magnetic Field Coils

A number of coils were placed on the upper and lower pole surfaces to allow slight modifications in the magnetic field. Coils of three turns each, which were formed to the shape of the electron orbits, were spaced 1/2-inch apart from 3 inches to 20 inches (on the hills). These coils are shown in Fig. 11. Three coils were also placed at each hill and valley; one set of hill coils is shown in Fig. 11. Measured along the center line of the hill, there was a coil (12 turns) from 10 inches to 14 inches, 12 turns from 14 inches to 18 inches, and another coil of 12 turns from 18 inches to 20 inches. A set of valley coils is shown in Fig. 12. From the outer radius inward they consisted of 39, 30, and 26 turns respectively. They were positioned radially to affect the same orbits as the corresponding coils on the hills.

All coils were of no. 21 magnet wire attached to brass sheets with Epon RN-48. The coil platters can be seen in place in Fig. 13. These auxiliary coils reduced the minimum gap by 1/2 inch, i.e., to 1.3 inches on the tops of the hills. A maximum of 1.5 amperes could be supplied to each coil through the control box of Fig. 14. Both the upper and lower coil currents could be adjusted in both current and polarity.

Radiofrequency System

The accelerating electrodes were three 60°-wide triants were situated in the valleys and separated from the ground sheets by 1/2-inch-thick teflon spacers. They extended radially from 2 inches to 20 inches. Figure 15 shows one of the electrode and ground sheet combinations. Fig. 16 shows this combination in place in the cyclotron. The upper and lower halves of each triant were tied together at radii of 2 inches and 20 inches except that the strap at 2 inches was removed for the threshold measurements. The system was tuned as shown in Fig. 17. The coarse tuning was accomplished with the inductive strap to ground, while a condenser outside the vacuum tank and connected to the triant through 18 inches of coaxial cable provided

the fine tuning. Also shown in Fig. 17 are the drive line and high-voltage phase pickup loop.

The voltmeter used a 9006 diode mounted on the ground sheet and connected to the electrode through a hole in the ground sheet. At low accelerating voltages the phase pickup connection was also made directly to the electrode. These two connections can be seen in Fig. 15 (top).

The triants were normally driven 120° out of phase but the phases could be adjusted as desired. The amplifier and phase-presentation apparatus was the same as was used with the earlier model, and provision was made to servo the phases with the same equipment used previously.

This electrode system was operated at 54.1 Mc and had a calculated energy gain per turn of 3 eV_0, where V_0 is the peak triant-to-ground voltage.

Electron Source

The electron source was similar to that used in the first electron model, a gain in radius of 0.080 inch being required for the first turn to clear the ground shield (Figs. 18 and 19). Electrons were injected with energies up to 2.5 Kev. Fig. 20 shows a source mounted on the source plug. The height, radius, and azimuth of injection could be adjusted from outside the tank.

Probes

Probe shafts of 3/4-inch stainless tubing could be introduced at several azimuths through locks and Wilson seals. Because of the size of the vacuum tank they were supported just outside the poles. For visual measurements the probe head was copper sheet with a thin coating of fluorescent powder.

For current measurements at large radii the collecting electrode was shielded with 1/4-mil Al foil. Bare probes showed no rf or spurious charged-particle pickup at radii between 7 inches and 18 inches.

OPERATION

In this section, all radial measurements refer to measurements on a hill, i.e. at 0°, 120°, or 240° unless otherwise specified.

Central Region

No attempt was made to investigate the starting conditions. Electrons were injected at radii of 1-1/2 inches to 3 inches with energies equal to the stable-orbit energies.

Region of Acceleration

Threshold voltage. As for the previous electron model, the threshold voltage was defined as the minimum peak accelerating voltage required to produce a current of 5×10^{-9} amps of electrons at full radius. This rather arbitrary definition was determined by the galvanometer sensitivities. Beam could be seen on fluorescent probes with currents smaller by a factor of ten. However, threshold measurements made by current and visual observations differed by less than 1/2 volt.

Although it is theoretically possible to calculate the form of the magnetic field required to make the periods of all stable orbits differ by less than any stipulated amount, the labor involved in the higher-order calculations is very great. The calculation of the present field was carried far enough that the maximum differences between the ideal and calculated periods of revolution were 0.1 percent or less.

As previously mentioned, the shimming of the magnetic field proved quite difficult, the actual and calculated fields differing by as much as 1 percent over large regions. No attempt was made to predict the threshold voltage from the field measurements.

The cyclotron was initially operated with no currents in the auxiliary coils--most of the electrons struck the upper pole at a radius of 5 inches. After small adjustments in the magnetic field had been made with the orbit coils a full-energy beam was immediately obtained with a peak triant voltage of 100 V.

Within a few days a threshold voltage of 24 volts was established. At 23 volts on the triants a small amount of beam was visible at all radii on a fluorescent probe. Below 23 V no electrons were able to clear the source

structure on the first turn. The voltage at which this occurred agreed well with the value calculated from the source geometry and the increase in radius of electrons in phase with the rf. The operating conditions for the threshold tuneup are given in Appendix III.

The measured threshold voltage was therefore determined by the source geometry rather than by the magnetic field. Extrapolating this figure to a 300-Mev deuteron accelerator of the same specifications, it is found that the threshold voltage would be less than 100 kilovolts.

It is interesting to note that if it is assumed that the electrons were in phase with the rf voltage, they made about 1,000 revolutions before reaching full energy. The actual number of turns was probably 2,000 or 3,000.

Axial focusing. With the cyclotron tuned up for minimum threshold voltage, the circulating beam was centered in the gap at all radii. The beam filled the gap at radii less than 5 inches, decreased in axial extent out to 10 inches, increased to 16-1/2 inches, and decreased slightly at larger radii (Fig. 21).

According to the adiabatic theorem, the axial amplitude should vary as $(\nu_a)^{-1/2}$. Using the calculated values of ν_a (Fig. 23) and normalizing at 10 in., the dashed line of Fig. 21 is obtained. The beam height clearly does not behave as expected, but it seems possible that the known magnetic field errors may be responsible.

The vertical focusing was also examined with the beam collimated axially from 3 inches to 5 inches. Hinged flags were fastened to the upper and lower ground sheets so that the size and axial position of the gap could be adjusted with an eccentric probe. A beam which was 1/8 inch high at 5 inches did not change much in appearance out to 16-1/4 inches on the hills, at which radius it was 3/16 inch high. At 18-7/8 inches the height was 1/4 inch, and the maximum extent was 1/2 inch in the beginning of the spill beam at 19-3/8 inches.

The effect of currents in the hill and valley coils is discussed in a later section.

Radial focusing. As previously explained, the magnetic field shape was designed to produce radial instability at $v/c = 0.49$, corresponding to a hill radius slightly greater than 18 inches. The predicted increase in radial amplitude was in fact observed, although it set in at a somewhat smaller radius. With no hill and valley coils on (the orbit coil settings are given

in Appendix III), the radial extent of the beam on a fluorescent probe was 1/8 inch out to 17-3/8 inches, where it started to grow rapidly. At 17-5/8 inches it was 1/2 inch; at 17-7/8 inches it was 1 inch. There was little change to 18-1/4 inches. Beyond 18-1/4 inches the radial lap on the hill probe was decreasing, and nearly all of the beam had left the cyclotron by 19-3/8 inches.

The effect of the hill and valley coils is discussed in the next section.

The effects of changes in the magnetic field on focusing. As the variation in the magnetic field around an orbit is increased, both the axial and radial focusing become stronger, the latter increasing at a faster rate. It was hoped that if the axial and radial focusing of the main field turned out as predicted, then by means of the auxiliary coils the point of radial instability could be pushed out to the edge of the cyclotron without increasing the axial extent of the beam very much. This could be accomplished by slightly increasing the field in the valleys and weakening it on the hills.

The qualitative behavior was as predicted: The radius at which the radial amplitude started to grow could be moved to smaller radii with an increase in the axial focusing, and vice versa. Two cases are given below. According to the data given in Appendix III, the currents used changed the hill field at 18 inches by 0.7 percent and the valley field at the radius corresponding to the same orbit by a like amount. Only the outermost hill and valley coils were used in these measurements:

(a) Upper and lower coils each 75 ma; hill coils negative field and valley coils positive: There was no increase in the radial extent of the pattern on the fluorescent probe at any radius. With vertical clipping at 5 inches, the height was 3/16 inch at 16-1/4 inches on the hills, grew to 5/8 inch at 18-7/8 inches, and remained fairly constant out to spill.

When the beam was not clipped at small radii the height was as indicated by (2) of Fig. 21. The beam almost filled the gap under these conditions, but there appeared to be no axial loss of electrons.

(b) Upper and lower coils each 75 ma; hill coils positive field and valleys negative: The beam was 3/16 in. high at 16 in., and did not increase in height at larger radii. The radial extent on the probe was 1/8 in. at 17 in., 1/4 in. at 17-3/8 in., and grew rapidly to a maximum of 1-1/2 in. at 18-1/8 inches.

The transition from circulating to external beam. The cyclotron was not intended to produce a well-collimated external beam without considerable modification in the shape of the magnetic field. However, the general characteristics of the spill beam may be noted:

(a) The last circulating orbits were centered in the cyclotron to within 1/8 inch.

(b) The pattern on fluorescent probes centered on the hills showed the strong axial focusing of the fringing field. Patterns on different hills were similar but not identical.

(c) Most of the beam emerged from the cyclotron in the valley following the hill (Fig. 22), rather than just before the center line of the hill, as in the previous model.

(d) With adjustment of the magnetic field about 1 percent with the large-radius hill and valley coils, nearly all of the external beam could be made to leave the poles in the valley following a single hill.

(e) Only electrons at radii of 19-1/4 inches or more on a hill could leave the poles in the next 120° of azimuth.

CONCLUSIONS

The performance of the machine was not exactly as predicted, but neither was the magnetic field shimmed to the accuracy specified, and it seems likely that Judd's calculations will accurately describe the behavior of a well-built cyclotron of this type.

To summarize some of the results obtained from this model:

1. The threshold voltage set by the magnetic field was not determined, but was less than 25 volts peak. This implies a minimum of 1,000 revolutions, and the actual number was probably several times this value.

2. The axial focusing at large radii was considerably weaker than predicted by the adiabatic theorem, but strong enough that no beam was lost into the poles or accelerating electrodes at large radii even for electrons started off the median plane.

3. The radius at which the predicted radial instability set in was somewhat smaller than the calculated value, but behaved as expected when slight modifications were made in the magnetic-field shape. In particular, when the hill fields were lowered about 1 percent and the valley fields raised a like amount over the last few inches of radius, the radius of radial instability could be moved to 19-1/4 inches on the hills without decreasing the axial focusing so much that the beam struck the gap-defining surfaces. Electrons at this radius should have speeds slightly greater than 0.51c. Inasmuch as the hill and valley coils allowed only crude adjustment of the large-radius field, a more carefully shimmed field could probably provide stable acceleration to the same energy with better axial focusing.

At the present time we see no reason why a satisfactory high-current cyclotron that could accelerate deuterons to energies slightly in excess of 300 Mev could not be built. However, additional work would be required to learn how to modify the magnetic field at large radii so as to extract a well-collimated beam. At this time we know that essentially all of the circulating current will emerge from the cyclotron without the use of additional deflecting systems, and that portions of the magnetic field can be modified so as to collimate this beam considerably.

It seems quite likely that considerably higher values of v/c might be obtained. In discussing this point it is useful to note the order of theoretical development of the ideas embodied in such accelerators. The original work of Thomas implied a general class of machines, but he carried out detailed calculations only to the lowest order in v/c, allowing no estimate of an upper limit to be made. A quite independent discovery of the same principle by Edwin McMillan in 1949 implied another general class of similar machines, containing rectangular rather than sinusoidal azimuthal field variations. However, the stability of specific members of this class can readily be calculated to give limiting values of v/c. McMillan considered both 3 and 4-section machines, and for the simplest ones obtained a maximum v/c of about 0.55. Judd studied the relationship between the work of McMillan and Thomas and calculated the more realistic sinusoidal field case in greater detail, especially for M = 3,* finding a similar limit at $v/c \simeq 0.55$. At this stage the concordant limiting values from two very different models seemed to discourage efforts aimed at increasing the limit.

The next development was due to J. R. Richardson, who undertook a careful study of more complicated and difficult examples of McMillan's class of machines with the hope of reaching higher energies. He was successful in showing that considerably higher values are possible for M = 4. His work led to further calculations by McMillan, which, after some lengthy numerical work by James Baker, resulted in a "theoretical" field shape with M = 4 becoming unstable at a v/c of about 0.7.

As this work took place at the close of the experimental program described here, the practical problems of obtaining the azimuthal variation required for M = 4 and the possibility of using even larger M values have not yet been evaluated.

---

*This work was concentrated on M = 3 for two reasons: (1) shaping pole faces appeared easier with 120° separation between hills, and (2) the theoretical pole face shape could be given by a simple analytical expression in this case but not for M = 4.

ACKNOWLEDGMENTS

Contributions to the construction and operation were made by the following:

Max E. Harris
P. T. Hibdon
Harry Keller
William Lawton
Minard Leavitt
Marvin Martin
Albert Proteau
Robert Ralston
Lazarus Ratner
Arthur Sherman
Robert Smith
Ferdinand Voelker
Dwight Vorkoeper

APPENDIX

I. The Choice of Constants in the Magnetic Field Expansion

The amount of axial focusing at the smaller radii is determined by the coefficient A. It can be shown that a necessary requirement for positive axial restoring forces is $A \geq 1.115$, the focusing being stronger for larger values of A. On the other hand, the larger the value of this constant, the smaller the radius at which the radial oscillations become unstable. A compromise value of A = 1.300 was chosen for this cyclotron.

The axial oscillation frequencies at large radii were then calculated for a number of choices of the coefficients C and E; some of the more promising cases are graphed in Fig. 22. (The amplitude of the axial oscillations is proportional to $(\nu_a)^{-1/2}$.)

To permit observation of the predicted radial instability at $\nu_r = 3/2$ ($\nu_r = \omega_r/\omega_0$), it was necessary to choose coefficients that would produce this phenomenon at about 1 inch less than the maximum possible radius. By trial and error it was found that C = 0.800 and E = 0.000 gave $\nu_r = 3/2$ at v/c = 0.490, corresponding to a radius of about 18-1/8 inches on the hills. As an example of how critical the shape of the magnetic field is, the coefficients A = 1.300, C = 0.800 and E = 0.500 would produce radial instability at v/c = 0.465 (17-1/4 inch radius). The difference between magnetic fields given by the two sets of coefficients is 0.5 percent at a hill radius of 18 inches.

Once the constants A, C, and E were chosen, the resonance condition was satisfied by calculating the other coefficients from:

$$B = 0.500 - 0.125\ A^2$$

$$D = 0.375 + 0.004018\ A^4 + 0.070312\ A^2 - 0.375\ Ac$$

and

$$F = -0.000549\ A^6 - 0.008301\ A^4 + 0.04353\ A^3c + 0.011742\ A^2 + 0.18751\ Ac - 0.250\ c^2 - 0.500\ AE + 0.3125$$

II. Construction of the Magnetometer Head

The magnetometer head is shown in Fig. 8. The circuit elements are imbedded in plastic at the center of the cooling-fin assembly. On the axis is a permalloy strip1 mil by 5 mils by 1/4 inch high. Wound about this strip are three coils:

1. rf input and d.c. bias current.
2. rf pickup.
3. Reverse d.c. bias current. This coil has half as many turns and twice the area of 1.

In operation, a rf signal is applied to coil 1. If the permalloy strip is in a magnetic field, a second harmonic of the rf signal will be generated and induced in coil 2. A d.c. bias current is then passed through coils 1 and 3 until the second harmonic signal becomes zero. The two bias-current coils provide a quadrupole field so that the bias current does not change the magnetic field in the iron of the poles.

This magnetometer head and the associated circuits were designed by Minard Leavitt along the lines of those commonly used for geophysical surveys.

III. Auxiliary Coil Settings and the Fields Produced by the Auxiliary Coils

The threshold measurements were made with the auxiliary coil currents of Table II.

Stable orbits were obtained to a hill radius of 19-1/4 inches ($v/c = 0.51$) with the auxiliary currents of Table III.

Table IV gives the fields obtained from radial runs on the hill (0°) and in a valley (300°) with the auxiliary coils set as in Table III. Also given are values of the field obtained from the theoretical expression. Note that these fields should not be identical at large radii. The theoretical field was designed to produce radial instability at 18-1/8 inches, whereas the measured field postponed the point of radial instability to 19-1/4 inches. To accomplish the latter, the hill field was lowered from 17-1/2 inches to 20 inches on the hills and raised from 15 inches to 17 inches in the valleys.

Tables V through VIII give spot-check measurements of the fields produced by some of the auxiliary coils. These measurements were made with the main field-coil current at the operating value, and with all auxiliary coils off except the one in question. The hill and valley coils are the outer coils, i.e. between 18 inches and 20 inches on the hill and 15-1/2 inches to 17-1/2 inches in the valley.

Table II

Auxiliary Coil Currents for the Threshold Voltage Measurements

Hill Radius	Upper ma	Lower ma	Hill Radius	Upper ma	Lower ma
2"	60	-75	15"	0	-10
3	-60	20	15-1/2	0	-10
3-1/2	0	-10	16	-10	0
4	0	-10	16-1/2	0	-10
4-1/2	25	0	17	10	0
5	-10	40	17-1/2	5	-10
5-1/2	0	-10	18	5	-15
6	-10	0	18-1/2	-15	10
6-1/2	35	35	19	-25	-20
7	0	-10	19-1/2	65	-105
7-1/2	0	-10	20	10	-20
8	-20	-30			
8-1/2	-35	-45			
9	5	-5			
9-1/2	0	-5	Electrons injected at		
10	-15	-25	1-3/4 inches at 650 volts		
10-1/2	0	-5			
11	5	-5			
11-1/2	-20	-15			
12	0	-5			
12-1/2	-5	0			
13	-15	-25			
14	-10	0			
14-1/2	0	-5			

Table III

Coil Settings for Radial Stability to 19-1/4 in.

Hill Radius	Upper ma	Lower ma	Outer Hill and Valley Coils	Upper ma	Lower ma
2"	85	85	$0^{o}H$	-70	-65
3	300	-300	$120^{o}H$	-80	-75
3-1/2	-70	80	$240^{o}H$	-80	-75
4	-10	5	$60^{o}V$	75	70
4-1/2	-5	0	$180^{o}V$	75	75
5	50	85	$300^{o}V$	80	75
5-1/2	0	-10			
6	-20	-35			
7	0	-10			
8	35	-10			
9	45	25			
13	-20	15			
14	-15	-30			
15	0	-5			
15-1/2	-5	0			
16	10	-15			
16-1/2	40	0			
17	0	-30			
17-1/2	-20	15			
18	15	-20			
18-1/2	0	-5			
19	0	-5			
19-1/2	15	15			
20	0	-5			

Table IV

Measured and Theoretical Fields in Percent of Central Field. Measured Values with Auxiliary Coils as of Table III

Hill Radius	0° Hill Theor.	0° Hill Meas.	0° Hill Dif.	300° Valley Theor.	300° Valley Meas.	300° Valley Dif.
4"	115.5	116.1	0.6	85.2	85.9	0.7
5	119.6	120.1	0.5	81.6	82.3	0.7
6	123.8	124.1	0.3	77.9	78.7	0.8
7	128.2	128.4	0.2	74.2	74.8	0.6
8	132.6	132.9	0.3	70.5	70.8	0.3
9	137.2	137.2	0	66.8	66.9	0.1
10	142.0	141.9	-0.1	63.0	63.0	0
11	147.0	146.8	-0.2	59.2	59.2	0
12	152.1	151.8	-0.3	55.3	55.3	0
13	157.5	157.6	0.1	51.3	51.5	0
14	163.1	163.0	-0.1	47.3	47.6	0.3
15	169.0	168.5	-0.5	43.2	43.5	0.3
16	175.1	175.6	0.5	39.1	39.2	0.1
17	181.6	180.6	-1.0	34.9	34.7	-0.2
18	188.4	187.6	-0.8	30.6	29.7	-0.9
19	195.5	192.8	-2.7	26.2	24.0	-2.2

Table V

Field Produced by 1200 ma in Upper and 1200 ma in Lower 17-inch Orbit Coils

Radius	0° Hill	330°	300° Valley
4"	0.69		0.52
10	0.83	0.61	0.36
14			0.19
15		0.49	0.05
16	1.00		-0.03
17	-0.19	-0.30	
18	-0.60		
19	-0.56		
20	-0.62		

Table VI

Field Produced by 1200 ma in Upper and 1200 ma in Lower 9-inch Orbit Coils

Radius	0° Hill	330°	300° Valley
4"	0.97		0.70
8	1.00	0.63	0.34
9	0.47	0.15	0.12
10	-0.07	-0.07	0
15	-0.17	-0.10	-0.05

Table VII

Field Produced by 500 ma in Upper and 500 ma in Lower 300° Valley Coils

Radius	0° Hill	330°	300° Valley
4"	-0.05		-0.02
10	-0.05	-0.04	-0.07
13	-0.05	-0.03	+0.07
14	-0.05	-0.03	0.22
15	-0.05	-0.03	0.35
16	-0.05	+0.12	0.50
17	-0.05	0.32	0.57
18	-0.05	0.23	
19	-0.05	0.04	
20	-0.08		

Table VIII

Field Produced by -500 ma in Upper and -500 ma in Lower 0° Hill Coils

Radius	0° Hill	330°	300° Valley
4"	0.04		0.03
13	0.05	0.03	0.02
15	0.02	0.05	0.01
16	0.06	0.01	0.01
17	-0.32	-0.08	0
18	-1.52	-0.14	
19	-1.27	-0.01	
20	-1.01		

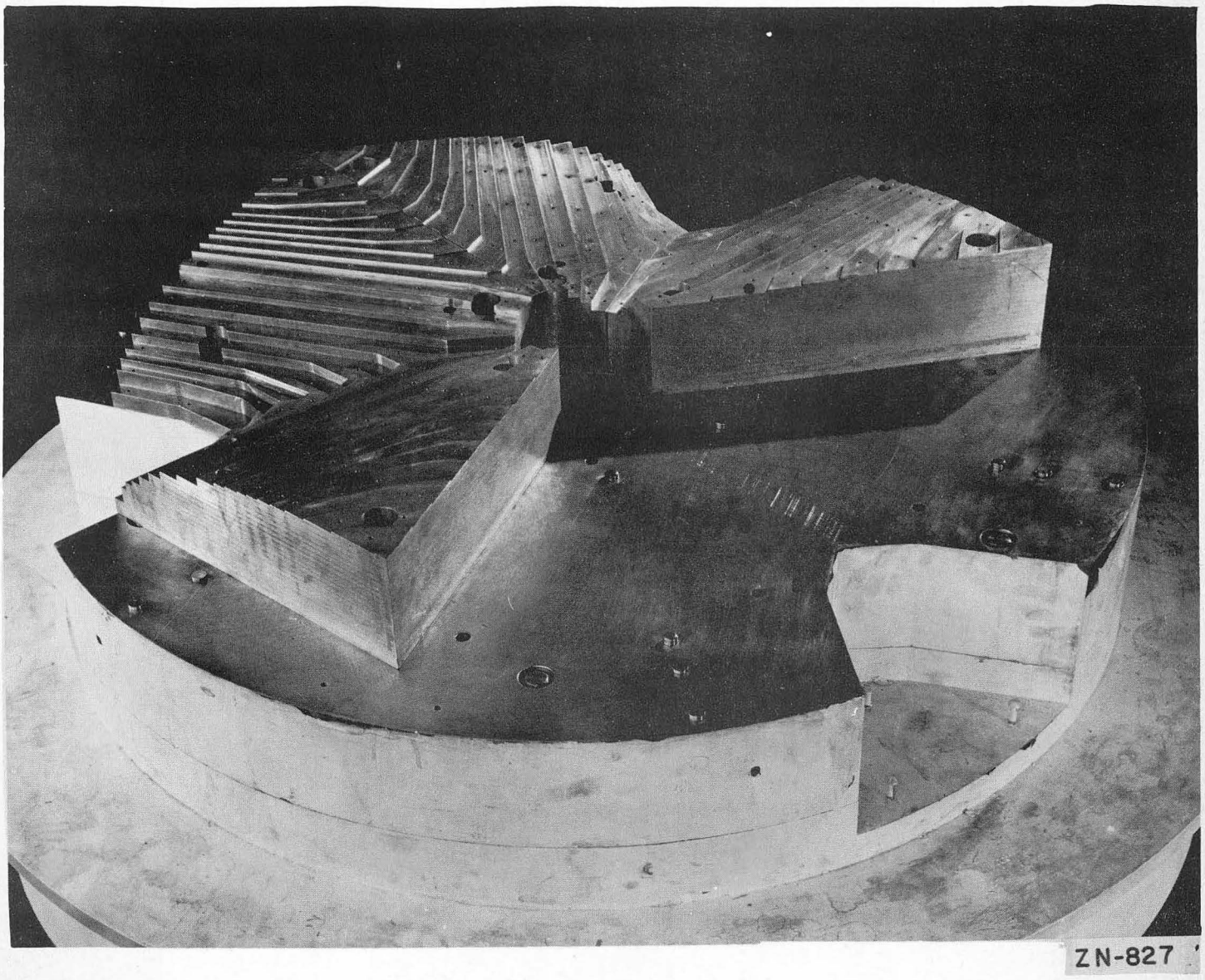

Fig. 1 Magnet assembly.

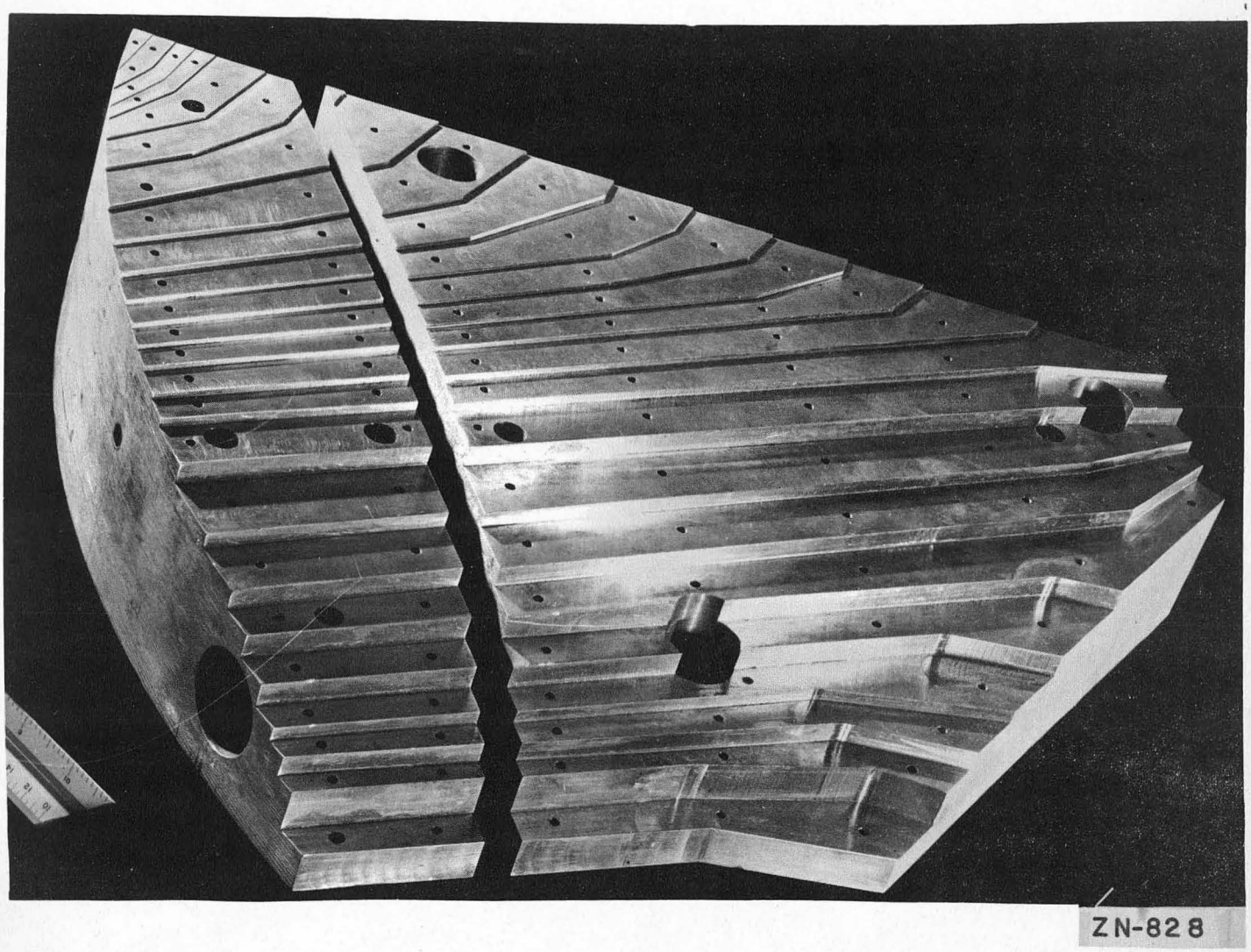

Fig. 2 Pole-tip sector.

Fig. 3 Assembled pole.

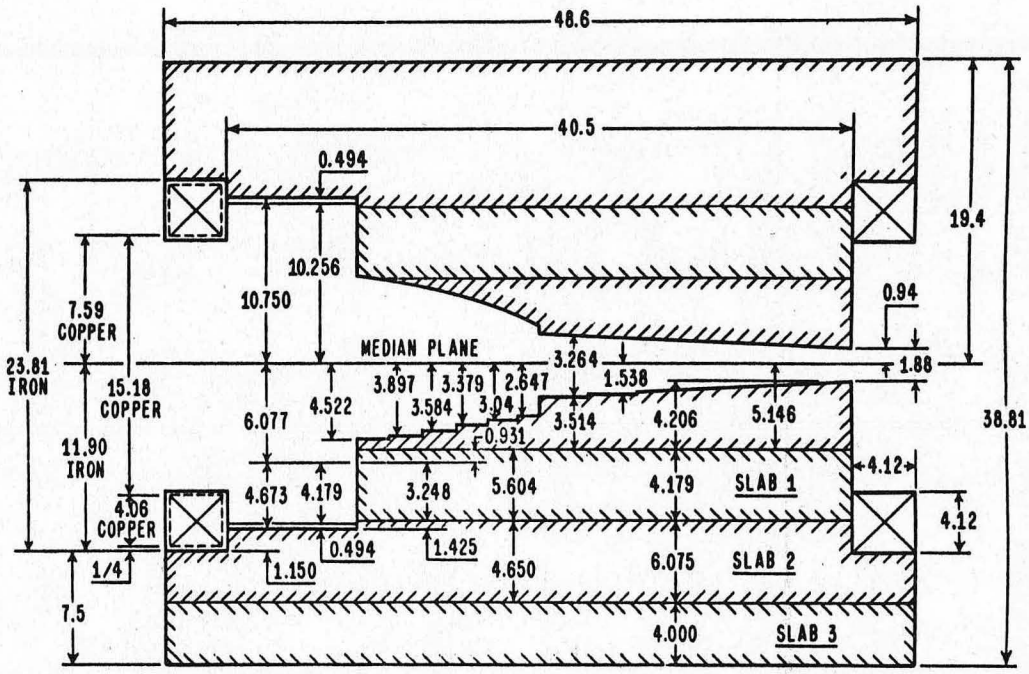

MAGNET CROSS SECTION.

MU-7085

Fig. 4

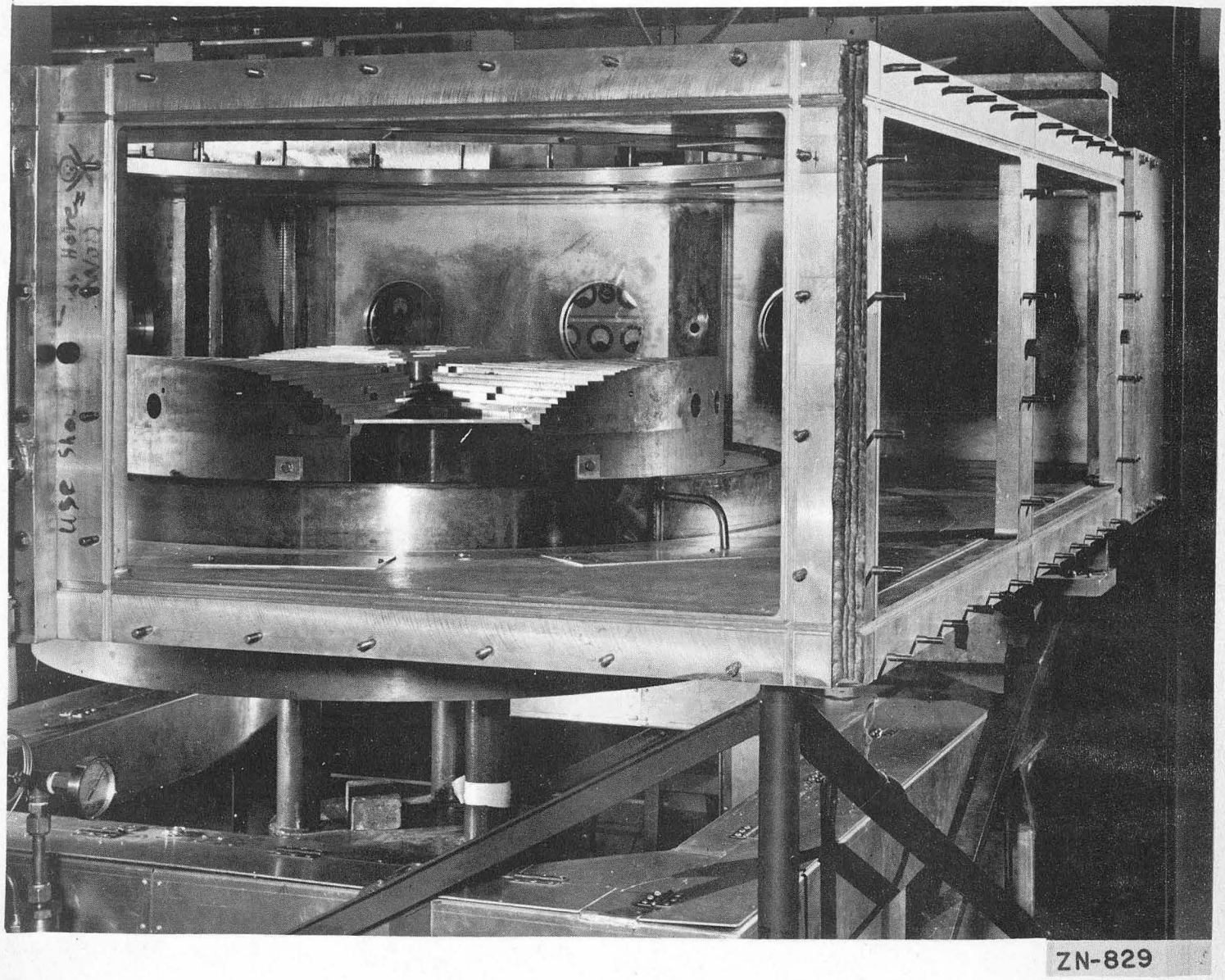

Fig. 5 Lower pole in vacuum tank.

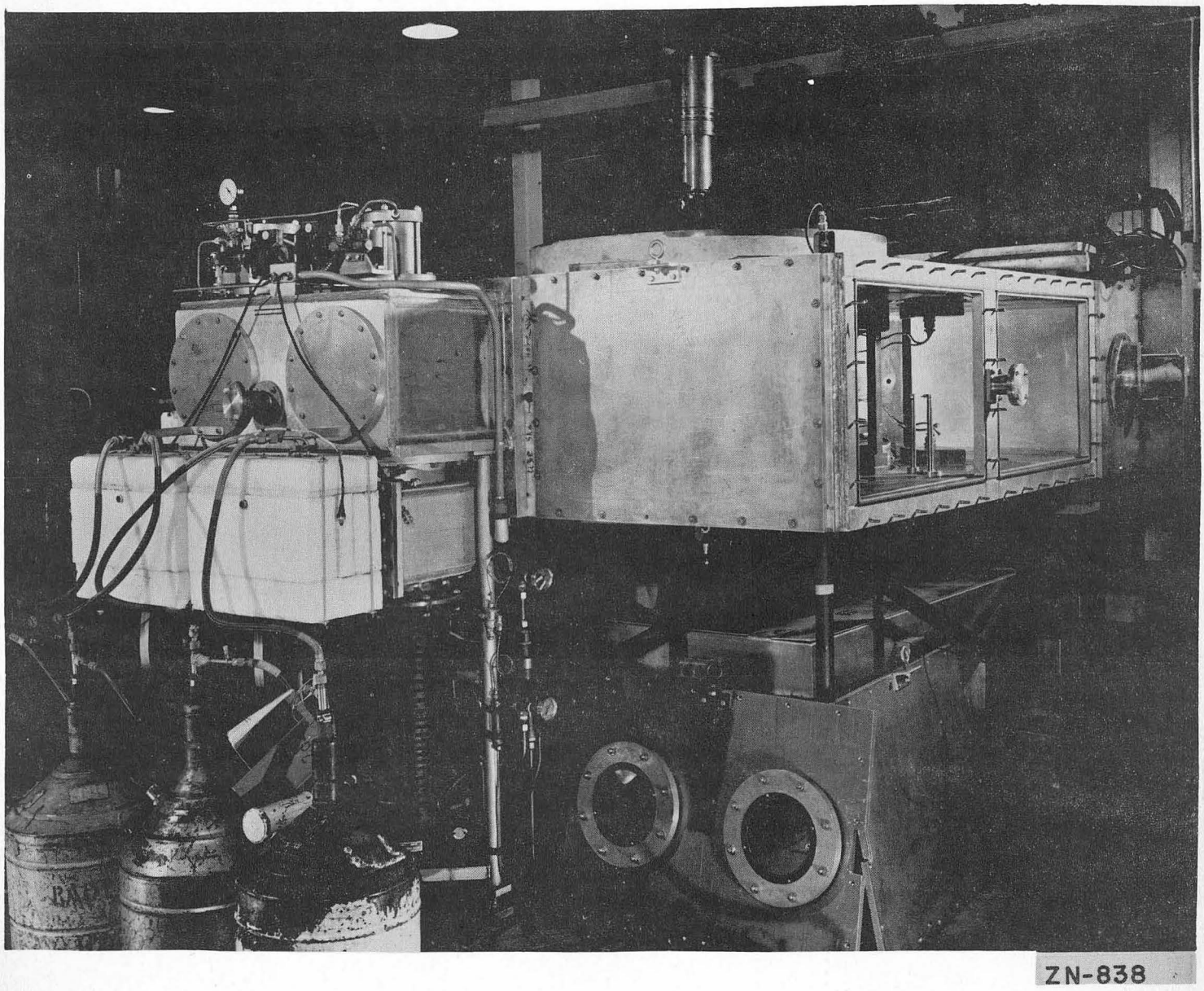

Fig. 6

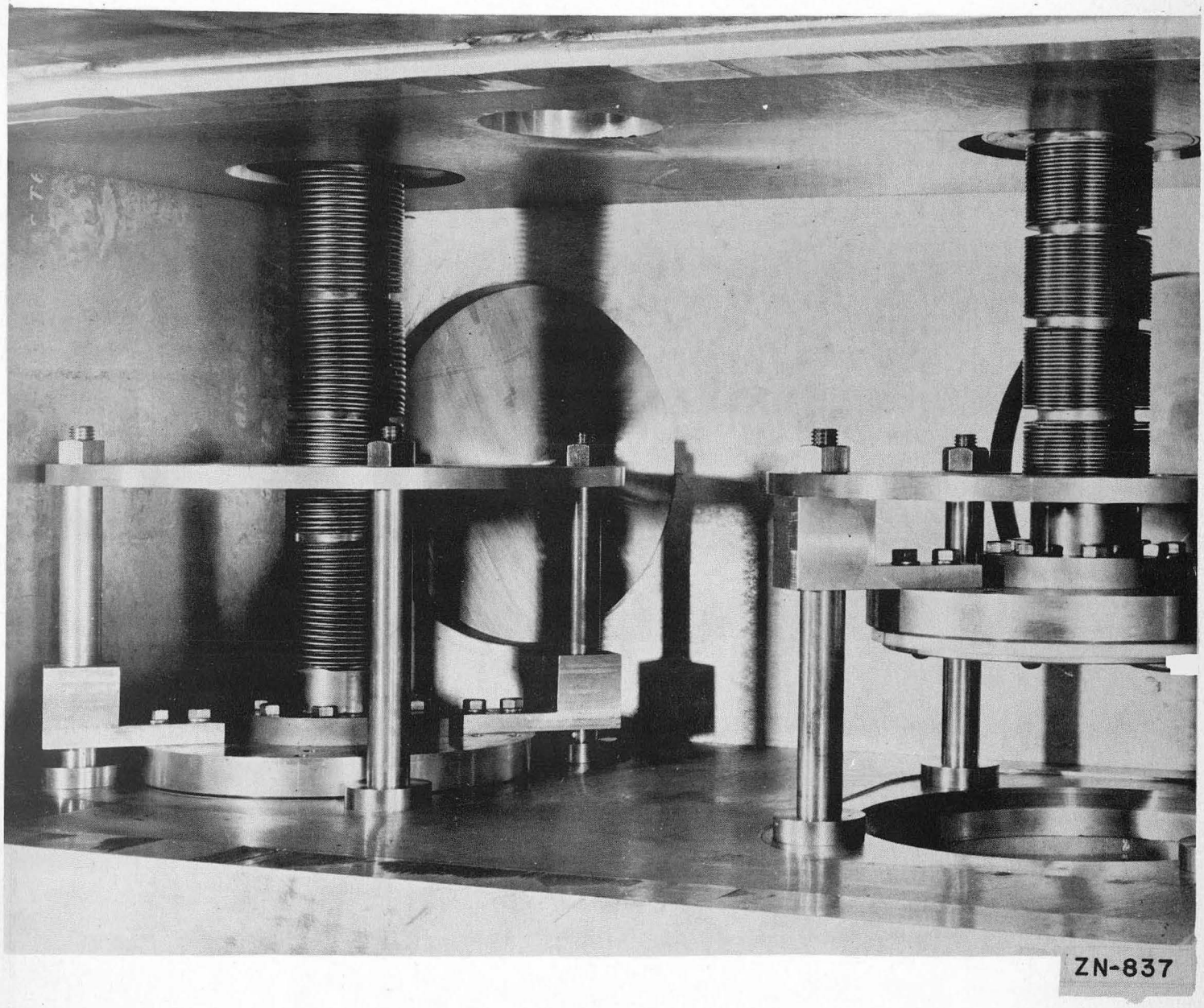

Fig. 7 Hydraulically operated diffusion-pump gates.

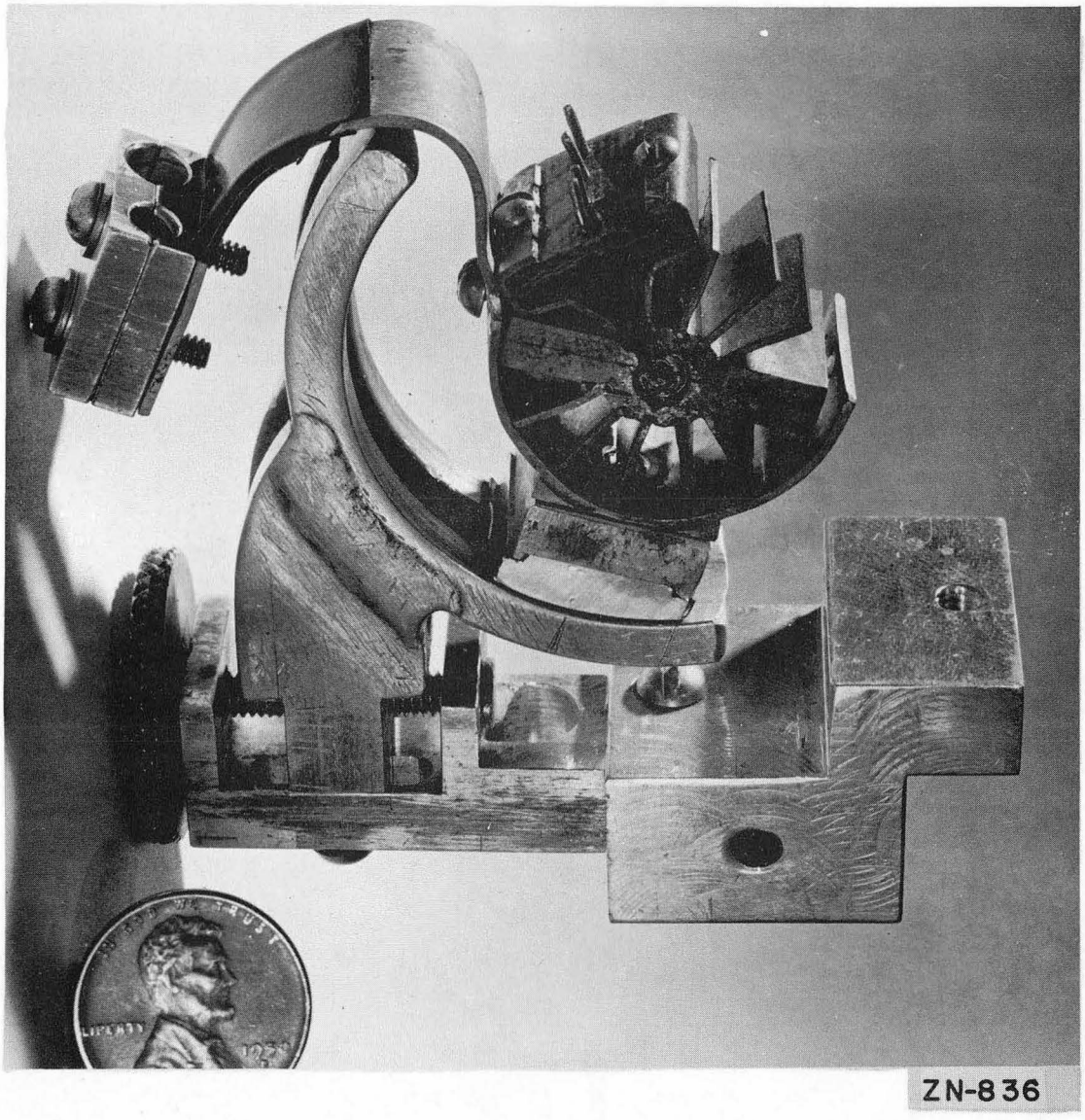

Fig. 8 Magnetometer head and carriage.

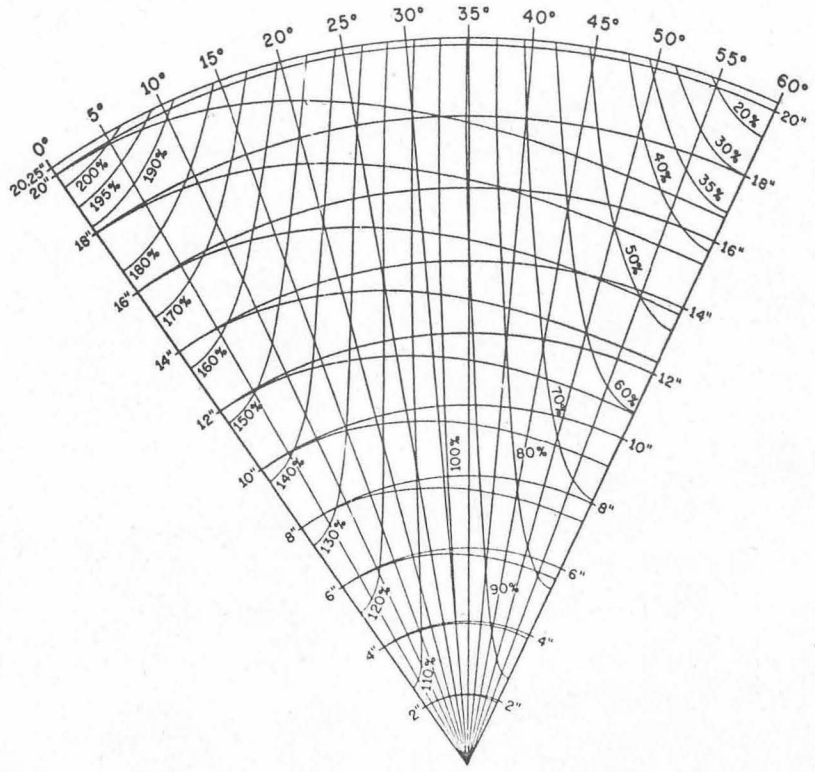

MAGNETIC FIELD CONTOUR LINES IN PER CENT OF CENTRAL FIELD. ALSO SHOWN ARE SOME CALCULATED STABLE ORBITS.

MU-7088

Fig. 9

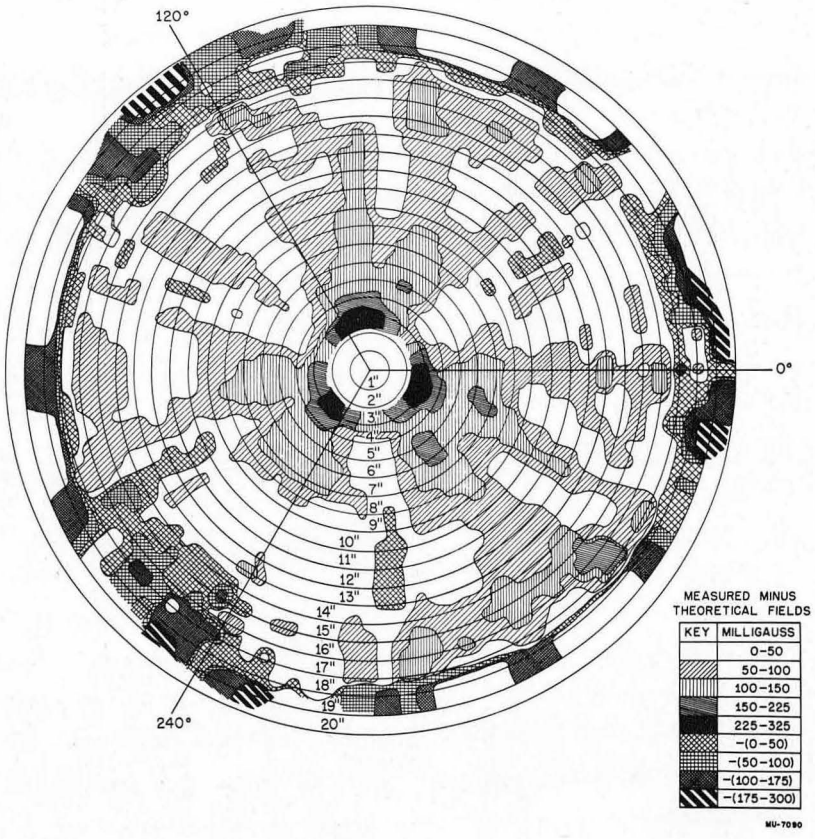
120°
0°
240°
1"
2"
3"
4"
5"
6"
7"
8"
9"
10"
11"
12"
13"
14"
15"
16"
17"
18"
19"
20"
MEASURED MINUS THEORETICAL FIELDS
KEY
MILLIGAUSS
0-50
50-100
100-150
150-225
225-325
-(0-50)
-(50-100)
-(100-175)
-(175-300)
MU-7090

Fig. 10

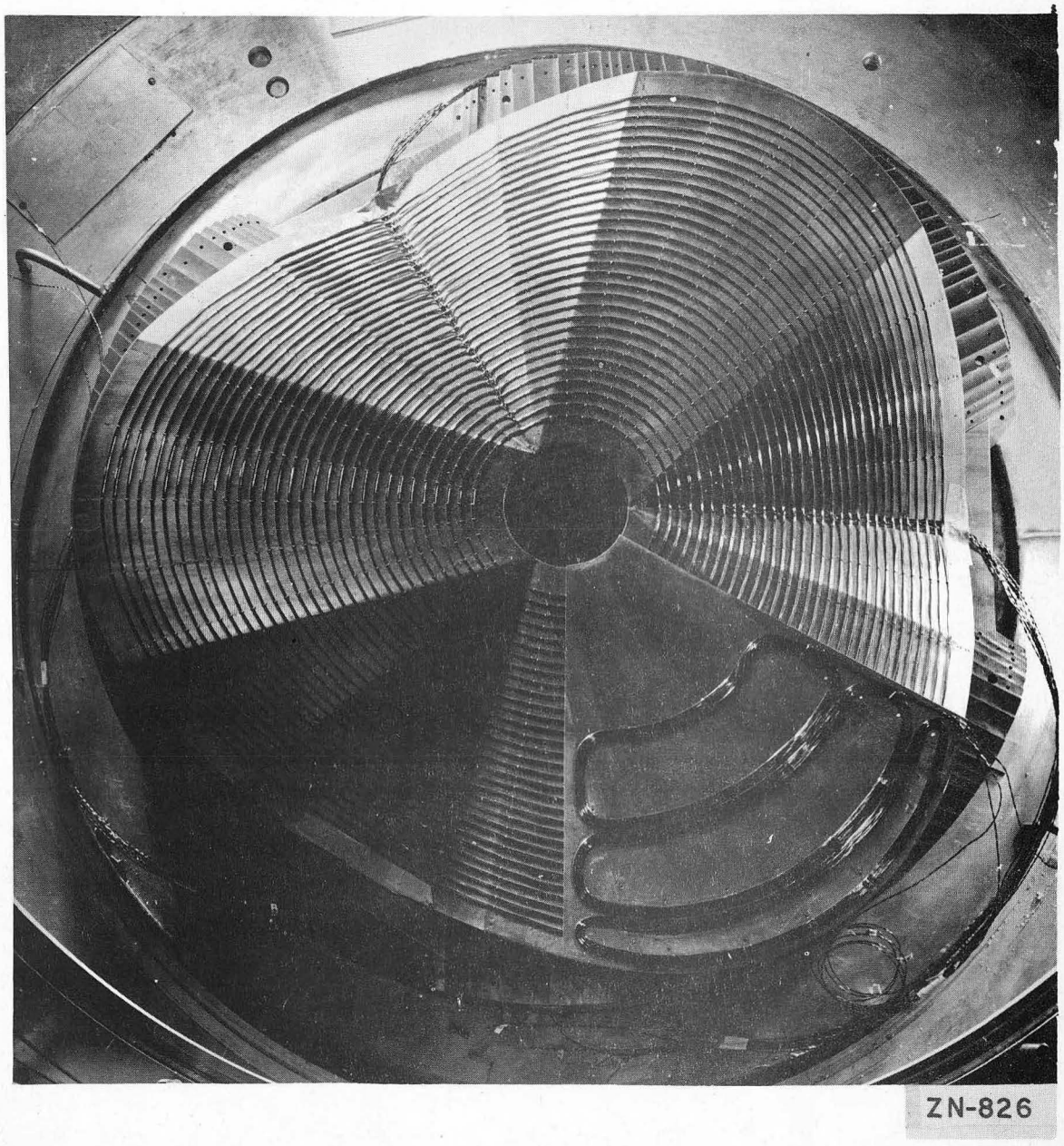

Fig. 11 **Orbit coils.** Three hill coils are also shown.

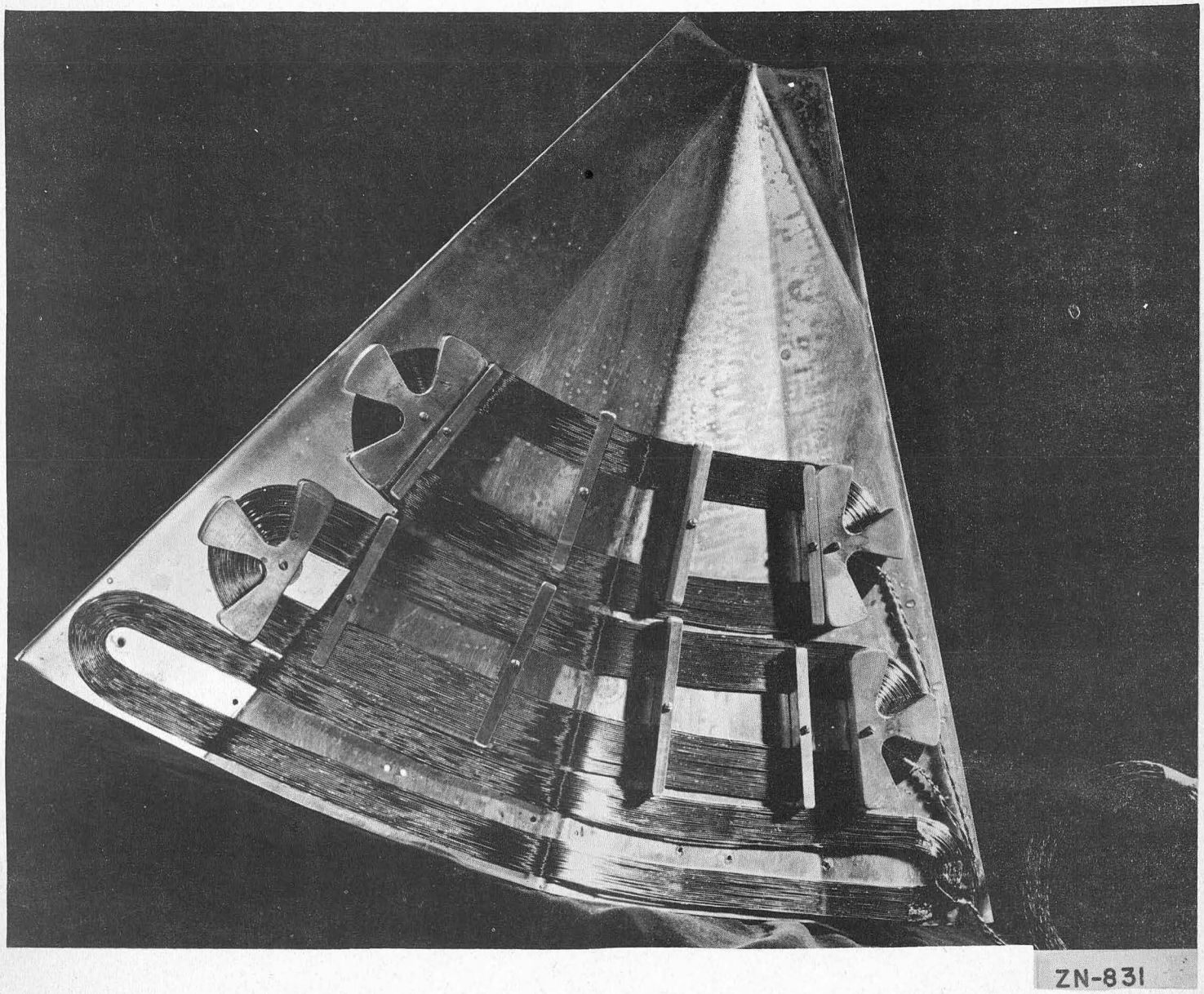

Fig. 12 Three of the valley coils.

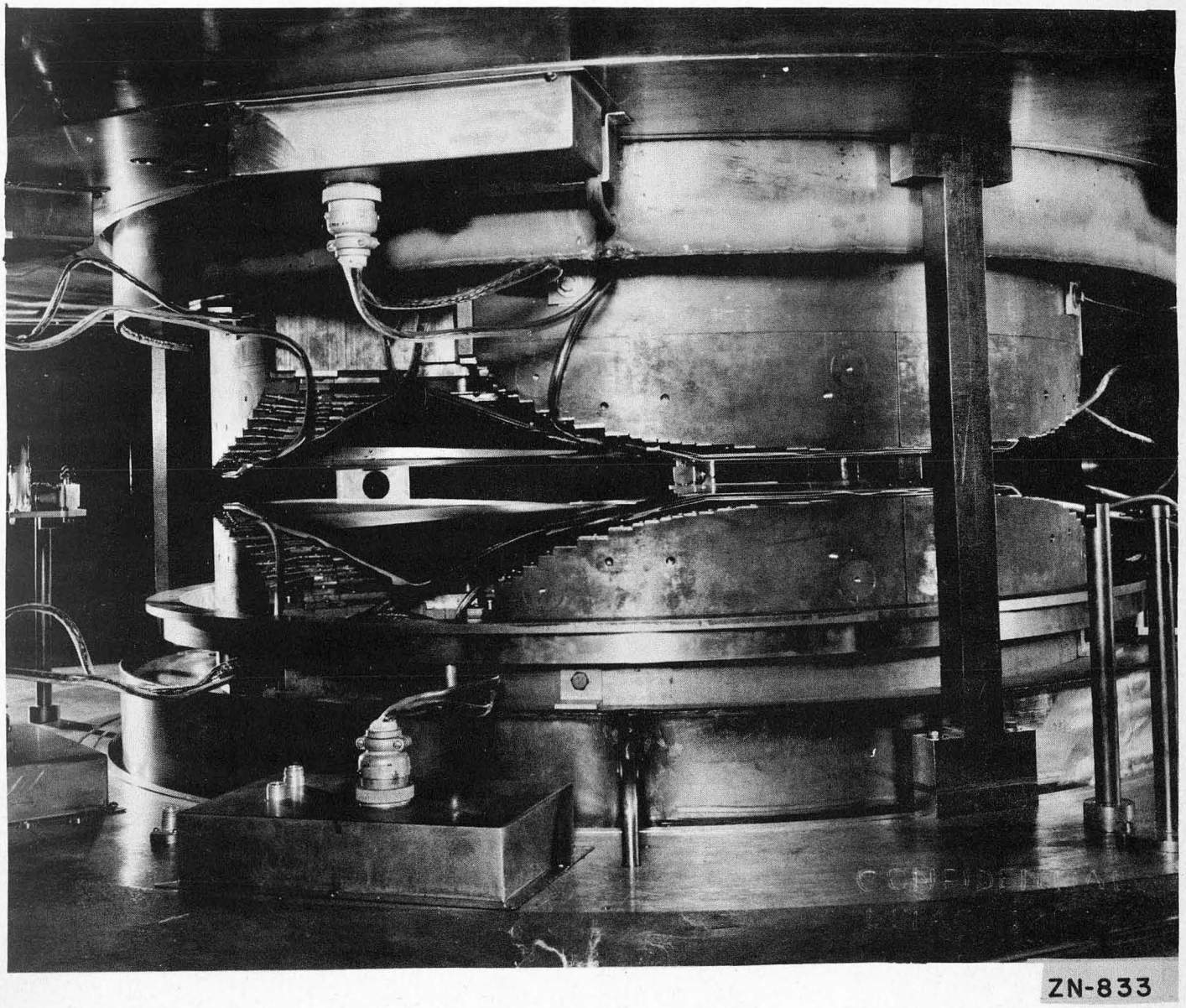

Fig. 13

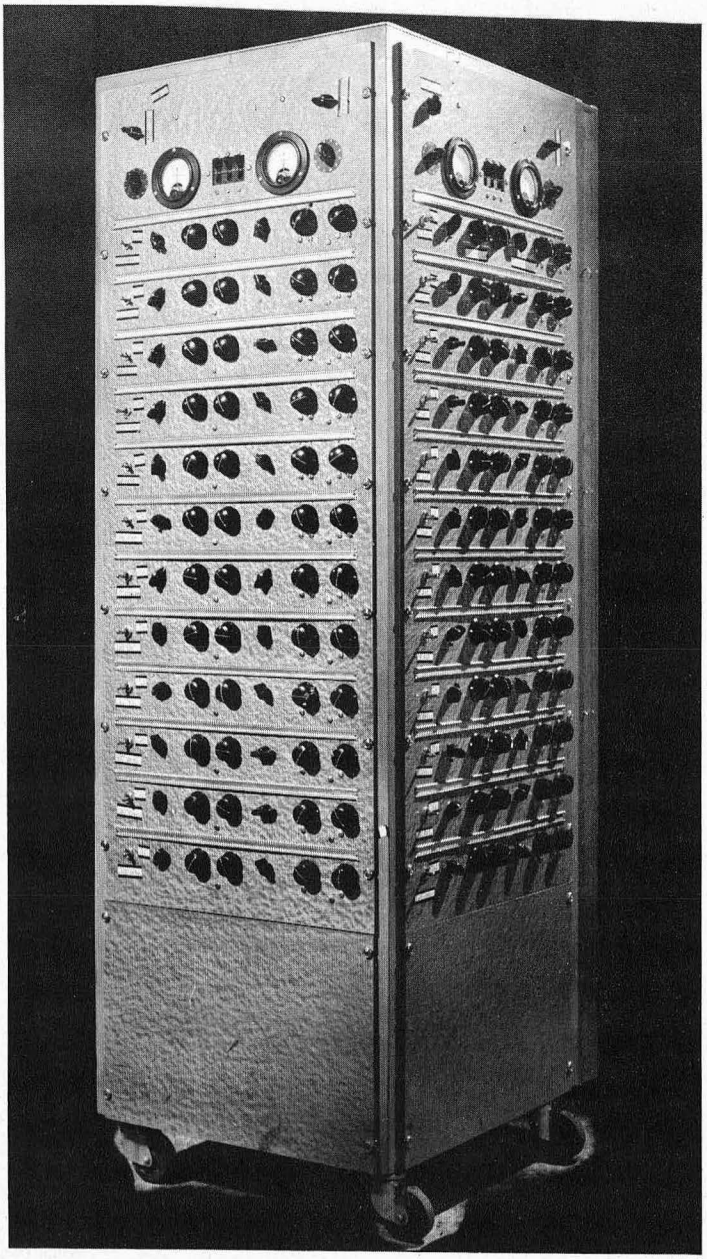

Fig. 14

ZN-720

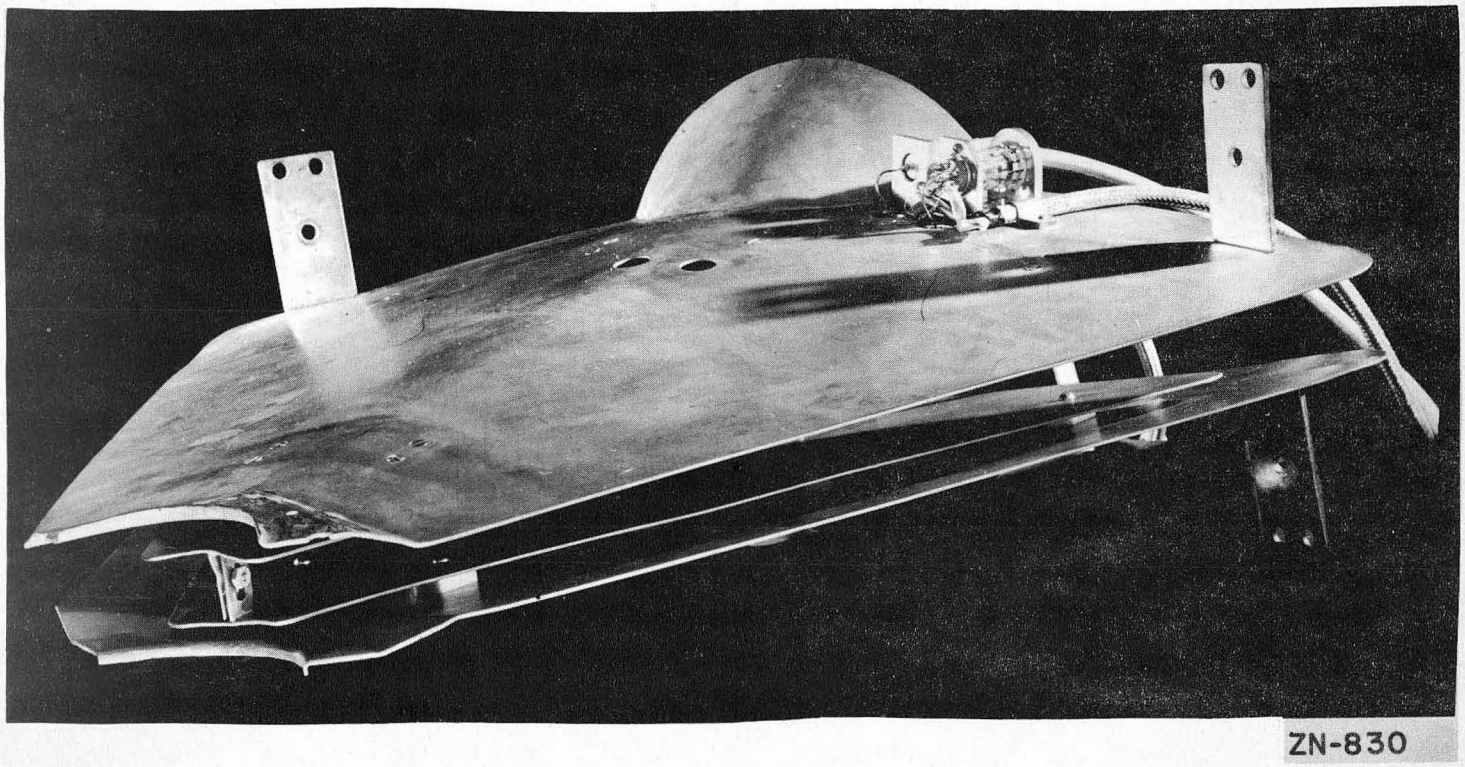

Fig. 15 60° triant.

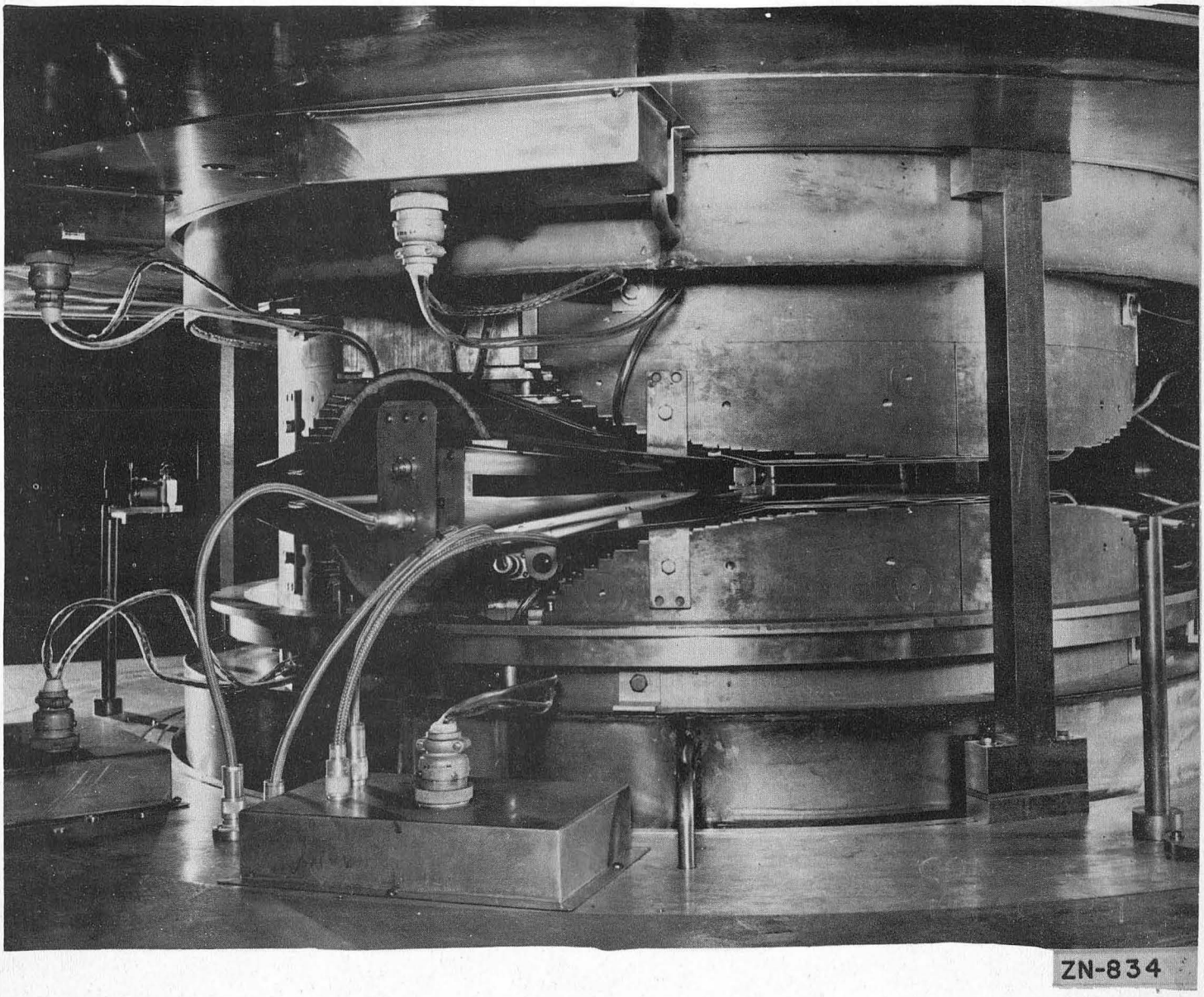

Fig. 16

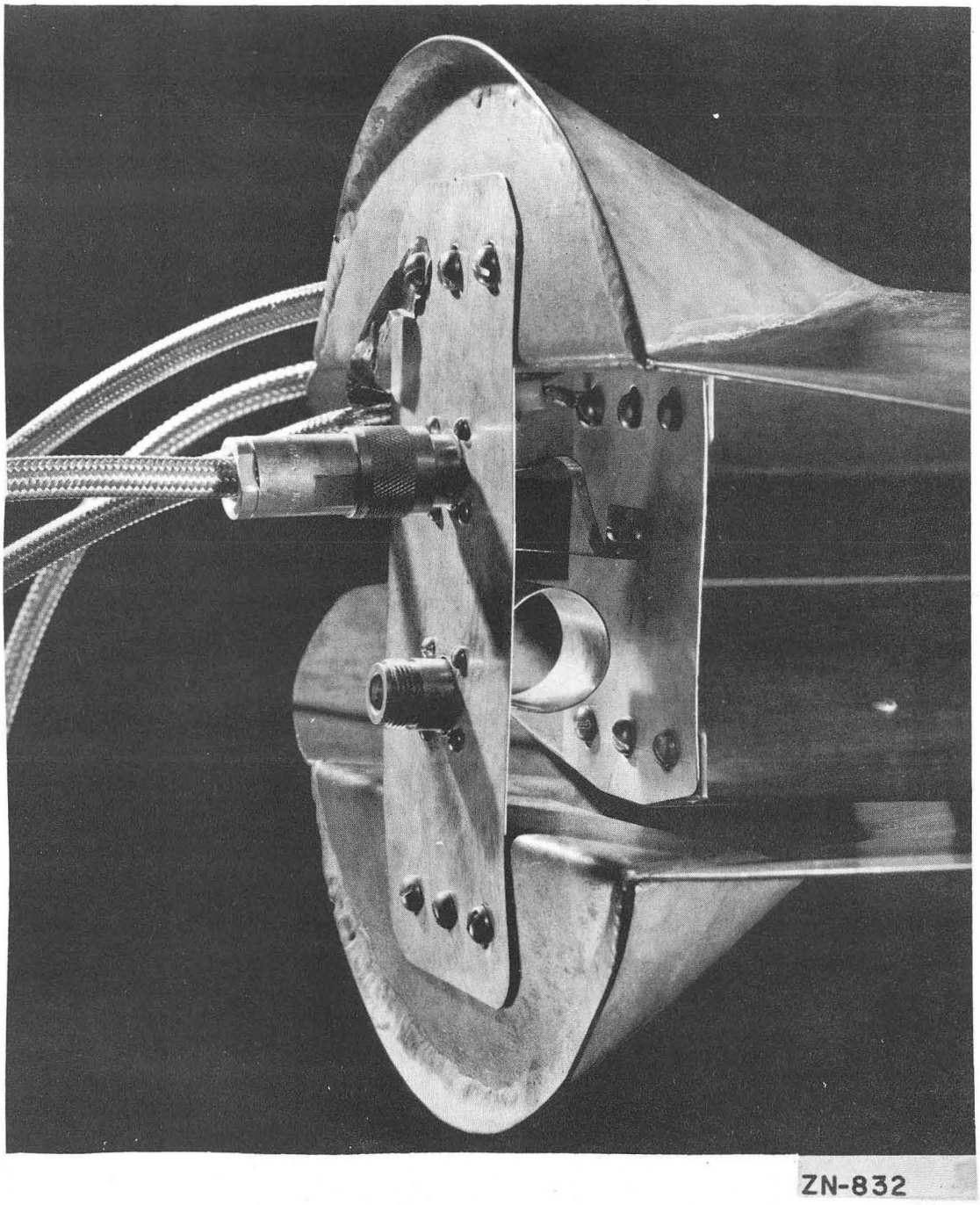

Fig. 17 Triant tuning and phase pickup structure.

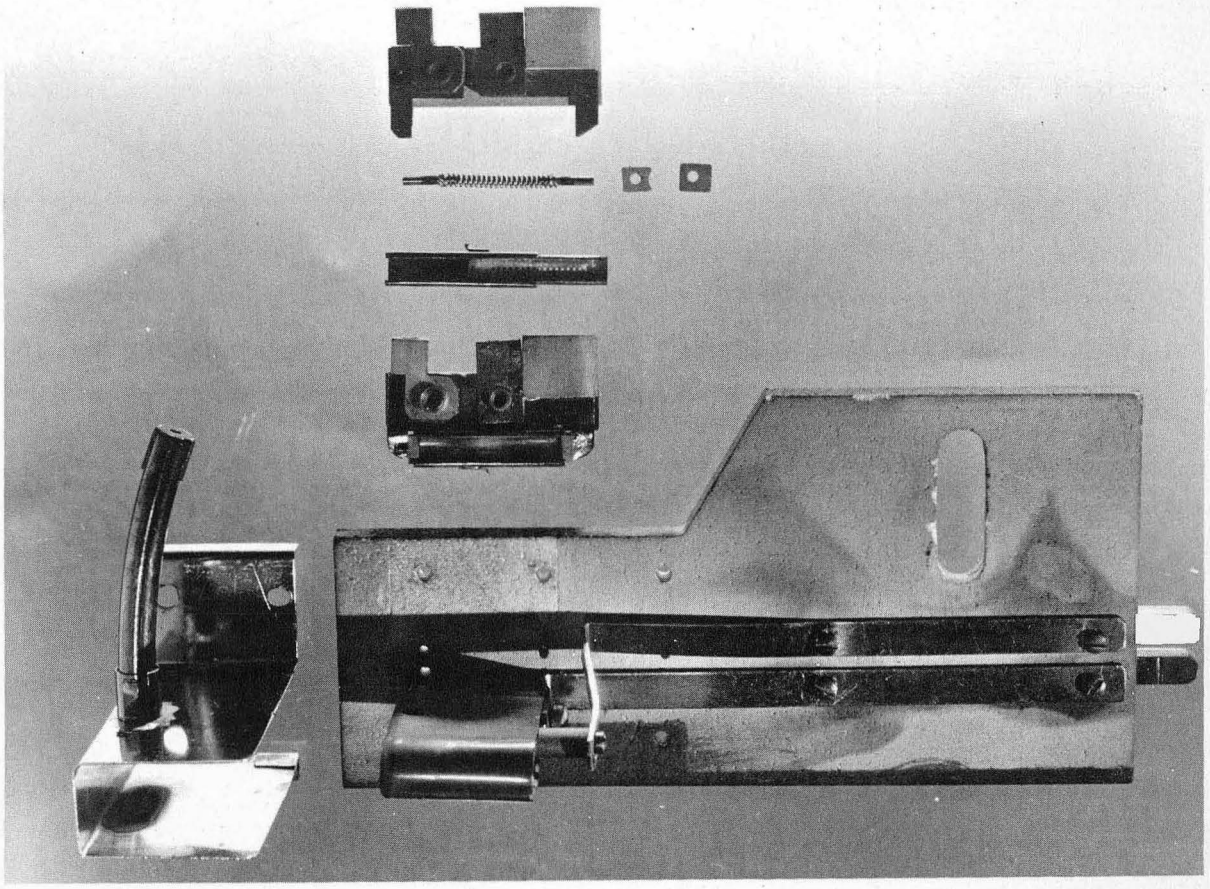

ZN-722

Fig. 18. Injection-type source with shield removed. Also shown are components of the emitting capsule.

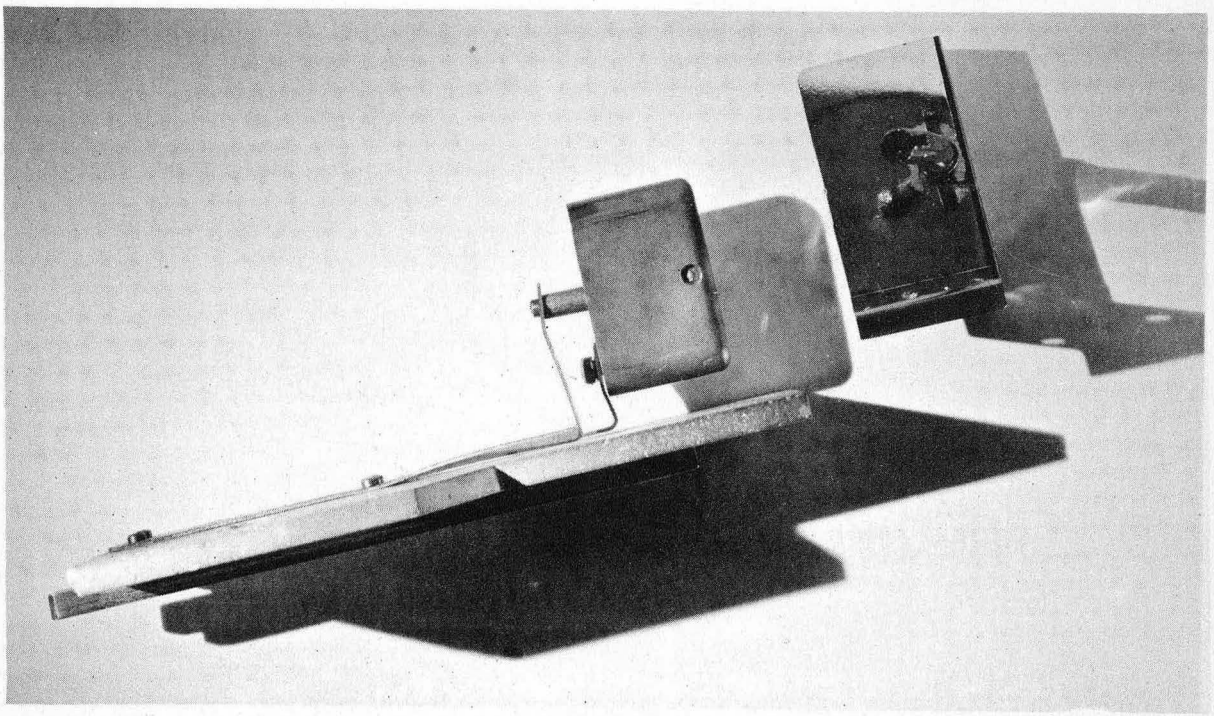

ZN-723

Fig. 19. Injection-type source with shield removed.

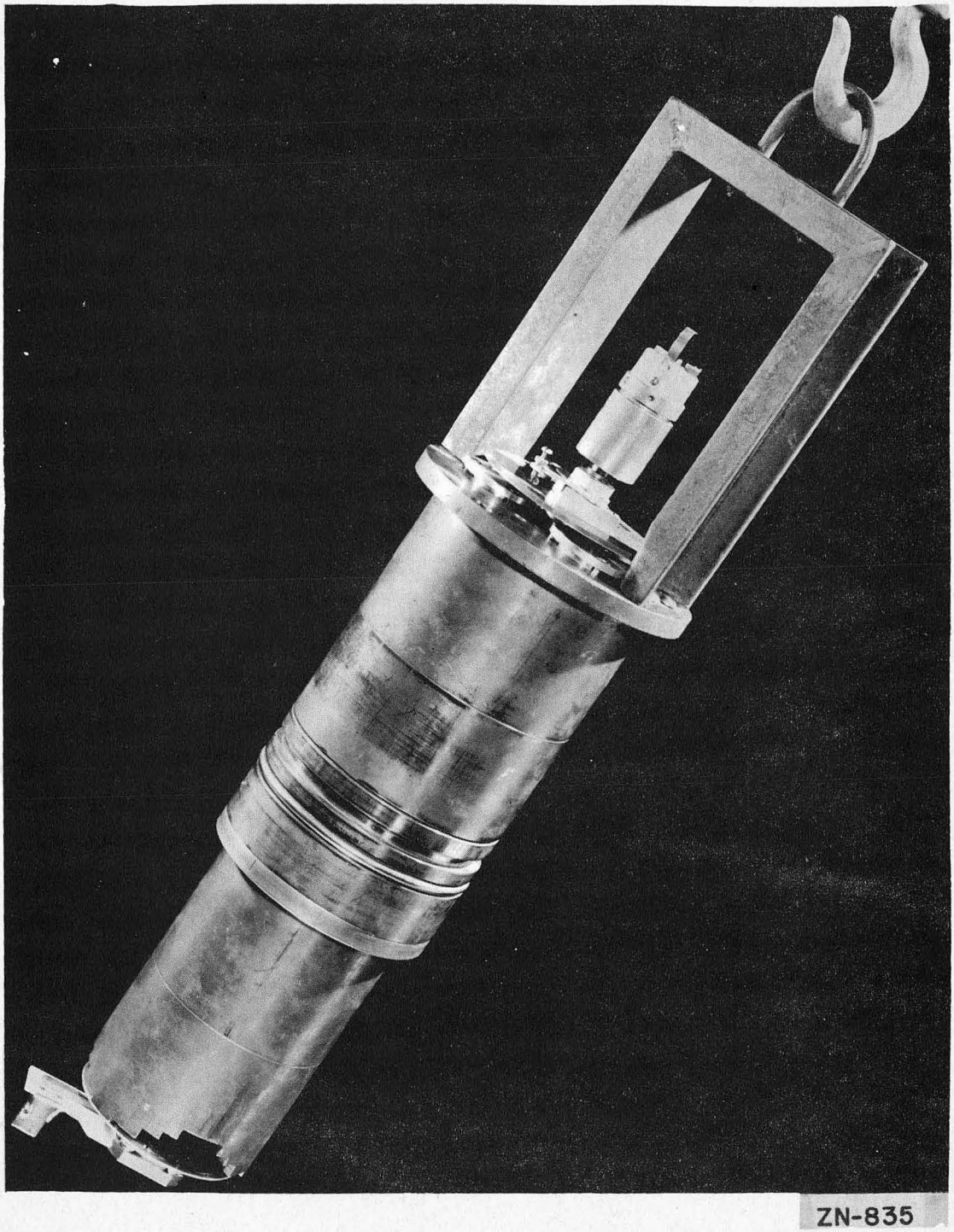

Fig. 20 Source mounted on plug.

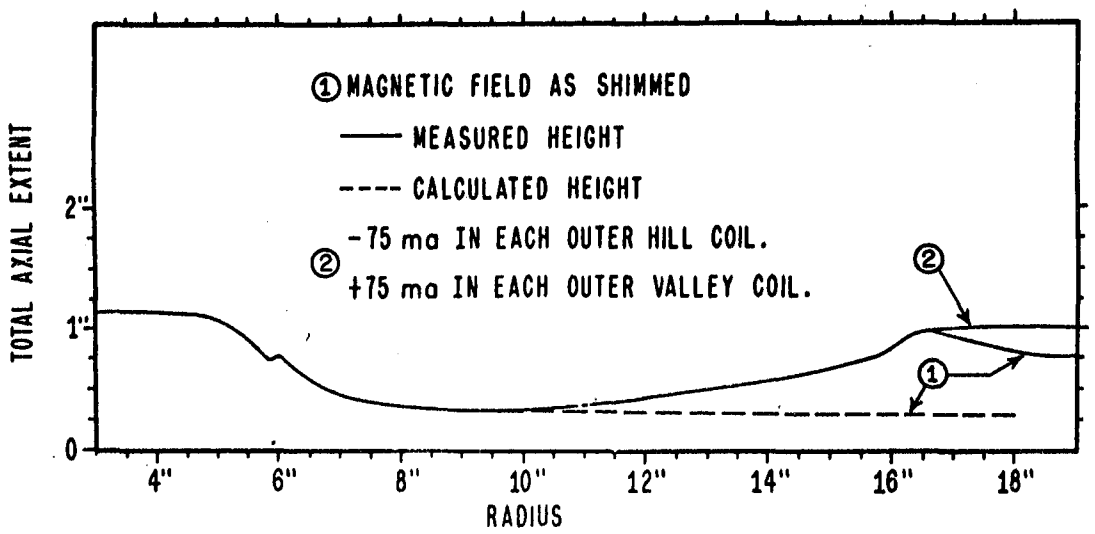

BEAM HEIGHT vs RADIUS.

MU-7088

Fig. 21

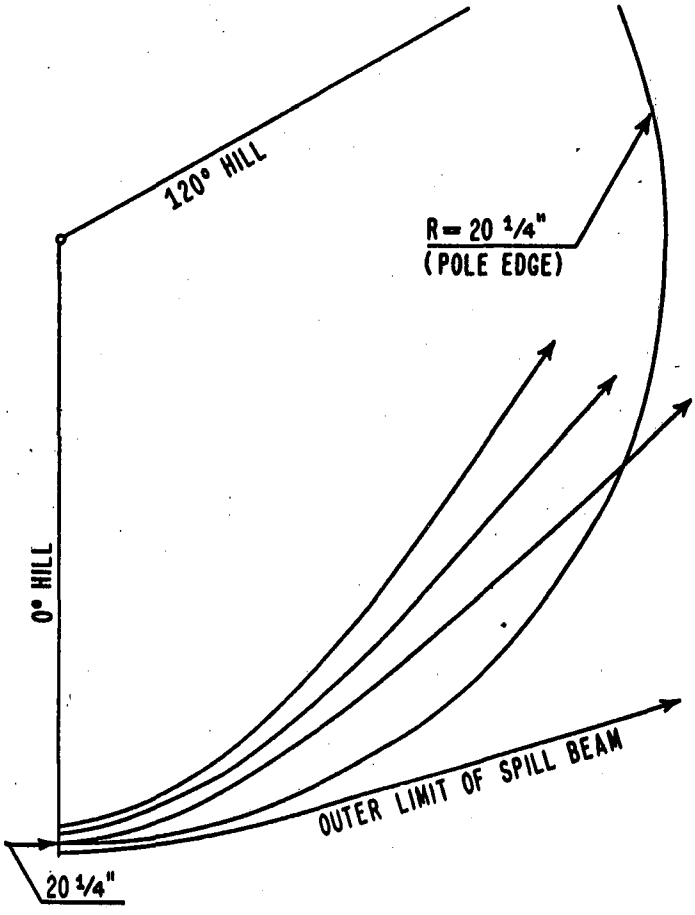

SKETCH OF SOME SPILL BEAM TRAJECTORIES.

MU-7086

Fig. 22

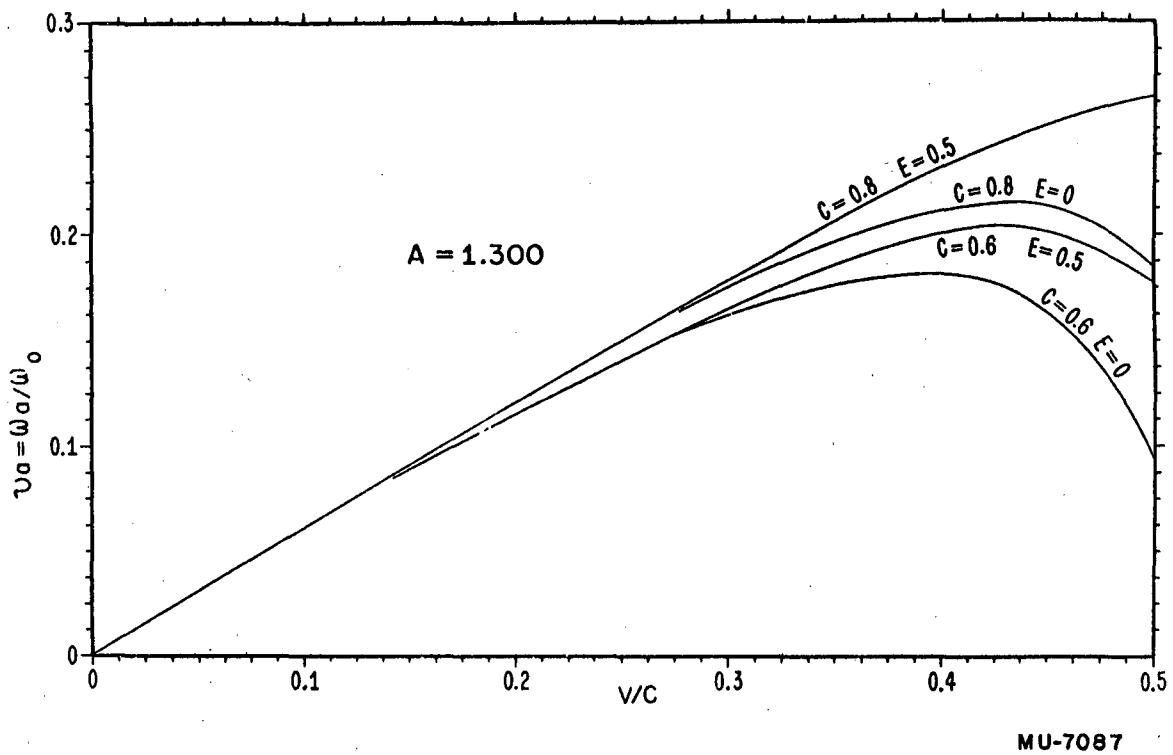
0.3
0.2
0.1
0
0
0.1
0.2
0.3
0.4
0.5
V/C
$\nu_a = \omega_a/\omega_0$
A = 1.300
C=0.8 E=0.5
C=0.8 E=0
C=0.6 E=0.5
C=0.6 E=0
MU-7087

Fig. 23